Aldhehyde Dehydrogenase Family-1 Regulates Female-Specific Visceral Obesity through mTORC1

A Senior Honors Thesis

Presented in Partial Fulfillment of the Requirements
for Graduation with Distinction
in Nutrition
at The Ohio State University

By
Barbara Reichert

The Ohio State University
June 2010

Project Advisor: Ouliana Ziouzenkova, Assistant Professor
Department of Human Nutrition

FULL TITLE:

ALDEHYDE DEHYDROGENASE FAMILY-1 REGULATES FEMALE-SPECIFIC VISCERAL OBESITY

ABBREVIATED TITLE: Vitamin A metabolism and female visceral obesity

AUTHORS' NAMES AND INSTITUTIONS: Barbara Reichert[1*], Shanmugam Jeyakumar[1,2*], Fangping Yang[1], Thomas Thomou[3], Rumana Yasmeen[1], Gabriela Orasanu[4], Molly Sharlach[4,5], Katharina S. Volz[1,6], Kari B. Green-Church[7], Hansjuerg Alder[8], Gregg Duester[9], Georgeta Mihai[10], Earl H. Harrison[1], Sanjay Rajagopalan[10], Jorge Plutzky[4], James L. Kirkland[3], and Ouliana Ziouzenkova[1#].

* These authors contributed equally to this work

[1]Department of Human Nutrition, Ohio State University, Columbus, Ohio, 43210, USA, [2]Biochemistry Division, National Institute of Nutrition, Jamai-Osmania, Hyderabad-500 604, India, [3]Robert & Alrlene Kogod Center on Aging, Mayo Clinic, Rochester, Minnesota 55905, USA, [4]Cardiovascular Division, Brigham and Women's Hospital, Harvard Medical School, Boston, Massachusetts 02115, USA, [5]Department of Plant and Microbial Biology, University of California, Berkeley, California, 94720, USA, [6]University of Graz, Austria, [7]Mass Spectrometry and Proteomics Facility, Ohio State University, Columbus, Ohio, 43210, USA, [8]Nucleic Acid Shared Resource, Comprehensive Cancer Center, Ohio State University, Columbus, Ohio, 43210, USA, [9]Development and Aging Program, Burnham Institute for Medical Research, La Jolla, California, United States, 92037, USA, [10]Davis Heart and Lung Research Institute, Ohio State University, Columbus, Ohio, 43210, USA.

THE ENDOCRINE SOCIETY NIH STATEMENT:

CORRESPONDING AUTHOR :

Ouliana Ziouzenkova, PhD

1787 Neil Avenue, 331A Campbell Hall

Columbus, OH 43210

Email: ziouzenkova.1@osu.edu

Telephone: 614 292 5034

Fax: 614 202 8880

KEY WORDS:

Retinaldehyde dehydrogenase, Raldh-1, rapamycin, proteomics, DIGE, insulin resistance, retinol, abdominal fat, alcohol dehydrogenases

GRANTS AND FELLOWSHIPS:

This research was supported by the American Heart Association SDG 0530101N and start-up funds (O.Z.); RO1 HL049879 and RO1 DK44498 (E.H.H), the US National Institutes of Health (R01 HL071745 and P01 HL48743) and the Donald W. Reynolds Foundation (J.P.), R01 EY013969 (G.D.), P30 CA16058-30 (Caliguiri)&NIH NCI OSU comprehensive cancer center support grant (K.B.G-C),

R01ES013406 and R01ES015146 (S.R), NIH grants AG13925 and AG23960 (J.L.K), the Ted Nash Long Life Foundation (J.L.K), and the Robert and Arlene Kogod Center on Aging (J.L.K), and ICMR-International Fellowship (S.M.J).

DISCLOSURE SUMMARY:

The authors have nothing to disclose

ABSTRACT

Diet and estrogen influence female visceral obesity by poorly understood effector mechanisms. Estrogen regulates the aldehyde dehydrogenase-1 family of enzymes (Aldh1A1, A2, and A3) that converts vitamin A metabolite retinaldehyde (Rald) to retinoic acid (RA). We hypothesized that this endogenous RA generation mediates sex-specific differences in visceral fat formation.

We identified Aldh1A1 as the major enzyme producing RA during adipogenesis in vitro and in mouse visceral fat in vivo. In high-fat-fed *Aldh1A1*$^{-/-}$ female mice compared to male groups, RA generation in visceral fat was impaired due to decreased *Aldh1A2*, and *Aldh1A3* expression. Accordingly, only female *Aldh1A1*$^{-/-}$ mice resisted diet-induced visceral obesity and glucose intolerance seen in WT mice. The glucose intolerance was transiently reversed by intraperitoneal RA injections into *Aldh1A1*$^{-/-}$ females.

Global proteomic comparison of WT and *Aldh1A1*$^{-/-}$ visceral fat revealed that *Aldh1A1*$^{-/-}$ mice had a subset of proteins changed in a sex-specific manner. Protein changes were mediated by mTORC1/p70S6K inhibition in *Aldh1A1*$^{-/-}$ females only. In consonance with mTORC1 inhibition, female, but not male *Aldh1A1*$^{-/-}$ mice had increased thermogenesis. Mechanistic studies demonstrated that RA activated and Rald inhibited mTORC1/p70S6K activation.

In the female model of visceral obesity induced by ovariectomy, Aldh1A1 deficiency also suppressed RA generation, inhibited mTORC1/p70S6K, and prevented visceral obesity. Similar mechanisms may be at work in women, who abundantly express Aldh1A1 in visceral adipocytes. Our data suggest a novel signaling role for Rald and RA in the regulation of sex-specific metabolic differences, and propose Aldh1A1 as a candidate target for treatment of visceral obesity in women.

INTRODUCTION

The female "thrifty" metabolism offered an evolutionary advantage during starvation. However, on a Western diet or after menopause, visceral obesity is prevalent in women (61.3% *vs.* 42%, in men) and increases their risks for type 2 diabetes, cardiovascular disease, cancer, and premature death (1-4). Visceral obesity is a polygenic and multifactorial disorder that is predisposed to by many systemic factors, including sex hormones (5). The preferential distribution of fat to visceral depots is characteristic of males; How a high-fat diet and decreased estrogen levels during the postmenopausal period promote visceral obesity in females is poorly understood (5, 6).

Vitamin A (retinol/ retinyl esters) and its metabolites regulate cell differentiation and metabolism through transcriptional mechanisms that involve specific nuclear receptors and various transcription factors (7-10). These functions are mediated by the three major vitamin A metabolites: retinol, retinaldehyde (Rald), and retinoic acid (RA) (9, 10). Less is known about the non-genomic role of retinoids (10). A recent report shows that stimulation of neurons with RA leads to rapid activation of the mammalian target of rapamycin (mTOR) (11), a serine/threonine protein kinase implicated in insulin signaling and regulation of translation by phosphorylation of p70S6 kinase and elongation factor binding protein (4E-BP1) (12). mTOR exists as two structurally and functionally distinct multiprotein complexes: rapamycin-sensitive mTORC1 and rapamycin-insensitive mTORC2. mTORC1 is also a well-established nutrient sensor that plays a key role in adipogenesis and diet-induced fat formation in rodents (13-15) and humans (16). Whether vitamin A metabolites regulate mTORC1 activation in obesity remains unknown.

Retinoid production and catabolism are controlled by different families of enzymes and binding proteins, which have distinct expression patterns in different tissues (8, 17). Rald is generated from retinol by alcohol dehydrogenases (Adh) and retinol dehydrogenases (Rdh). RA is produced solely from Rald by the cytosolic aldehyde dehydrogenase-1 family of enzymes (Aldh1 also known as Raldh). The expression of vitamin A-metabolizing enzymes is under spatiotemporal endocrine control including influences by sex

hormones (8). Estrogen suppresses *Aldh1A1* and increases *Aldh1A2* expression in the uterus (18, 19); dihydrotestosterone and RA activate *Aldh1A3* expression (20). These Aldh1 enzymes may control equilibrium between Rald and RA. In pharmacological treatment with retinoids, both Rald and RA regulate adipogenesis and fat formation (21-24). Altered vitamin A homeostasis can also have a marked impact on the development of obesity (23, 25-27). Deficiency in Rald-generating enzymes facilitates diet-induced obesity (25, 26). In contrast, increased Rald levels in *Aldh1A1*$^{-/-}$ mice render them resistant to diet-induced obesity (23). Numerous and somewhat controversial data in diet-induced obesity models, leave many questions unanswered regarding the role of vitamin A metabolism in the regulation of fat distribution between subcutaneous and visceral depots or sex-specific effects in adipose tissue.

Here, we provide evidence that sex-specific expression of the Aldh1 enzymes alters RA generation, thereby orchestrating visceral fat formation in a sex-specific manner.

RESULTS

Aldh1A1 deficiency results in sex-specific formation of visceral fat

To test whether Aldh1A1 influences sex-specific differences in fat formation we analyzed WT and *Aldh1A1*$^{-/-}$ male and female mice on regular chow and after 180 or 300 days on a high-fat diet (**Figure 1A**). Both WT and *Aldh1A1*$^{-/-}$ female mice weighed less than male mice on a regular chow diet. On a high-fat diet, WT females and males had similar weight. Food and water intake was similar between males and females of both genotypes on a high-fat diet (**Figure 1B**). WT females, however, accumulated more fat than WT males, specifically in visceral (perigonadal) depots (**Figure 1C, D;**). The *Aldh1A1*$^{-/-}$ female mice gained significantly less weight than males due to marked suppression of visceral fat formation (**Figure 1A, D; Supplementary Figure 1A, B**). The longer HF feeding (180 vs.300 days) further suppressed visceral depot mass in *Aldh1A1*$^{-/-}$ mice and this proceeded in sex-specific fashion (**Figure 1, A, D; Supplementary Figure 1B**). The increase in visceral fat on a high-fat diet was

associated with large adipocytes in all groups, with the exception of *Aldh1A1*$^{-/-}$ females, which maintained small adipocyte size (**Figure 1D**). The *Aldh1A1*$^{-/-}$ females were also significantly more glucose tolerant than *Aldh1A1*$^{-/-}$ male mice (**Figure 1E**). Thus, diet-induced fat formation in *Aldh1A1*$^{-/-}$ mice was impaired in a sex-specific fashion, namely, female mice resisted visceral obesity more than male mice.

Aldh1A1 deficiency impairs RA generation in female but not in male mice

Given the known role of Aldh1A1 in RA production from Rald (23, 28), we examined whether Aldh1A1 deficiency influences the expression of vitamin A metabolizing enzymes in visceral fat (**Figure 2A**). WT males and females had similar expression of Rald-generating *Adh* enzymes (**Figure 2B,** left panel). In *Aldh1A1*$^{-/-}$ mice, the expression of *Adh* enzymes in visceral fat was not altered compared to WT mice, with the exception of decreased expression of *Adh3* in *Aldh1A1*$^{-/-}$ males. Overall *Adh3* expression was relatively low compared to the abundant *Adh1* enzyme. Expression of *Rdh10* and *Rdh1* as well as *Aldh8a1* enzymes did not differ between groups (Fig. 2B and **Supplementary Figure 1B,C**). Short-chain dehydrogenase/reductase and aldo-keto reductase enzymes were not examined in this study.

In contrast to similarly expressed *Adh* enzymes, RA-generating enzymes from the Aldh1 family had markedly different expression in WT males and females, which was especially evident in *Aldh1A1*$^{-/-}$ mice (**Figure 2B,** right panel). *Aldh1A1* was expressed at higher levels than the other *Aldh1* enzymes in visceral fat of WT male and female mice. *Aldh1A2* and *Aldh1A3* expression was lower in WT females than in WT males. Both *Aldh1A2* and *Aldh1A3* expression were lower in *Aldh1A1*$^{-/-}$ females than in males, with *Aldh1A1*$^{-/-}$ females having the lowest expression of RA-generating *Aldh1* enzymes. Consistent with this, expression of the RA receptor target gene *Cyp26A1* was significantly lower in *Aldh1A1*$^{-/-}$ females compared to WT females (6.6% vs.100%) (**Figure 2C**). *Cyp26B1* was expressed at similar levels in all groups (**Figure 2C**). We also examined differences in RA production in visceral fat,

using cell lines that expressed a luciferase reporter construct containing RA response element (RARE) (**Figure 2D**). In consonance with known selective activation of RARE by retinoic acid (9), in our assay, RARE activation induced by Rald was 100 times lower than that of RA (based on EC50), in keeping with prior data in transiently transfected cells (29). To investigate whether decreased expression of Aldh1 enzymes in *Aldh1A1*$^{-/-}$ female mice is associated with decreased RA production, we extracted lipophilic compounds from visceral fat and stimulated RARE-expressing cells with these extracts. The validation of the RARE assay and plasma retinol concentrations are shown in **Supplementary Figure 2A, B**. The lowest RARE reporter activity was associated with lipid extracts from visceral fat of *Aldh1A1*$^{-/-}$ females (81% compared to RARE activation from WT females) (**Figure 2E**).

To show that such a moderate decrease in RA concentrations has an impact on metabolic processes in *Aldh1A1*$^{-/-}$ females, RA was injected intraperitoneally into the *Aldh1A1*$^{-/-}$ females followed by a glucose tolerance test 10 min after injection (**Figure 2F, left panel**). The treatment with RA in the *Aldh1A1*$^{-/-}$ females was sufficient to significantly impair glucose tolerance compared to *Aldh1A1*$^{-/-}$ females injected with vehicle. Nonetheless, even in the presence of RA, *AldhAa1*$^{-/-}$ remain more glucose tolerant than WT females. To support the presence of RA in circulation 10min after its intraperitoneal injection we stimulated RARE-expressing cells by plasma of RA- and mock-injected mice (**Supplementary Figure 2C**). The RARE was significantly activated by plasma of RA-, but not mock-injected animals. In contrast, intraperitoneal injection of Rald to WT females partially improved glucose tolerance in these animals (**Figure 2F, right panel**).

Aldh1A1 deficiency results in sex-specific changes in proteins in visceral fat

To define mechanisms by which sex- specific production of RA in *Aldh1A1*$^{-/-}$ mice influences visceral fat, we performed a comparative proteomic analysis of visceral fat in WT versus *Aldh1A1*$^{-/-}$ mice in male and female groups (**Supplementary Figure 3**). DIGE analysis of the proteome revealed 13 proteins that

varied significantly in abundance in visceral fat from WT versus *Aldh1A1*$^{-/-}$ mice after false discovery rate correction (FDRC) of 176 and 167 proteins in male and female groups that were different between WT and *Aldh1A1*$^{-/-}$ mice without FDRC. **Table 1** shows the proteins that changed significantly by DIGE analysis: 1) in both male and female groups (e.g. Group 1*'Significant in both groups in proteomic analysis'*); 2) only in male groups; and 3) only in female groups. Among identified proteins were Atgl, Serpina3a, a paralog of vaspin, and caspase1. Previous reports have implicated PPARγ, RXR or their ligands, such as glitazones and RA, in the regulation of these genes (30-33). We analyzed mRNA expression of all proteomic marker genes from Table1 (last four columns) and established genes related to PPARγ and RXR pathways (*Fabp4* and *leptin*) in visceral fat from each mouse group (**Supplementary Figure 4**). Quantitative examination of mRNA expression of all proteomic markers showed significant differences in the expression of many genes in the WT and *Aldh1a1*$^{-/-}$ groups (Table 1, Group 3; Supplementary Fig. 4, *caspase1*). Three markers, *Glod4*, *Tgh,* and *leptin*, were differentially expressed in the female groups of WT and *Aldh1A1*$^{-/-}$ mice; *Vaspin* was differentially expressed in the WT and *Aldh1A1*$^{-/-}$ male groups. However, none of the proteomic markers was expressed in a sex-specific fashion in *Aldh1A1*$^{-/-}$ male and female groups. Thus, despite the significant differences in protein levels in visceral fat, the changes in mRNA expression of proteomic markers were not sex-specific within the *Aldh1A1*$^{-/-}$ group (Table 1, last column). Our subsequent experiments elucidated mechanisms that mediate sex-specific differences in protein, but not in mRNA expression in *Aldh1A1*$^{-/-}$ mice.

Among proteins significantly changed in the female group in DIGE was a major adipose triglyceride lipase and PPARγ target gene, Atgl (30, 34). Quantitative analysis of visceral fat from the same mice revealed that *Atgl* mRNA expression in visceral fat was similar in all groups (**Figure 3A**), whereas Atgl protein levels were significantly higher in *Aldh1A1*$^{-/-}$ females compared to all other studied groups (**Figure 3B**). To examine whether this regulation pattern depends on the decreased RA generation from Rald seen in *Aldh1A1*$^{-/-}$ females, we stimulated differentiated 3T3-L1 adipocytes with retinoids (100nM)

(**Figure 3C**). We observed a significant increase in Atgl protein levels upon stimulation with Rald, whereas RA and retinol did not influence Atgl levels. A possibility that mTORC1, a known mediator of protein translation induced by nutrients (15, 35), can affect Atgl protein levels in adipocytes was tested in differentiated 3T3-L1 adipocytes treated with rapamycin (**Figure 3D**). Rapamycin increased Atgl protein levels in a dose-dependent manner (**Figure 3D**). The effect of RA and Rald on the activation of mTORC1 was further examined in HEK293 cells (**Figure 3E**). RA stimulation (100nM) significantly increased insulin-mediated phosphorylation of p70S6K, an mTORC1 downstream target. In contrast, the same Rald concentration suppressed this effect in HEK293 cells (38.9% vs. 100% in cells stimulated with insulin alone).

Aldh1A1 deficiency suppresses mTORC1 activation in vitro and in vivo

Next, we elucidated the putative link between vitamin A metabolism and mTORC1 regulation in vitro in differentiated 3T3-L1 adipocytes. Among Rald-generating enzymes, *Adh1* (306%) and *Adh3* (143%) were expressed at higher levels in differentiated versus non-differentiated pre-adipocytes (**Figure 4A**). *Rdh10* expression was lower in differentiated (59%) than in non-differentiated pre-adipocytes; *Rdh1* and *Adh4* expression was very low and did not change during differentiation. Among RA-generating enzymes, *Aldh1A1* was the only enzyme induced significantly during differentiation (201%, $P<0.035$); moreover, *Aldh1A1* had the highest expression level among Aldh1 enzymes (**Figure 4B**). The mitochondrial *Aldh2* and *Aldh8A1* are inefficient at Rald oxidation and were not studied here (8). Since *Aldh1A1* was the most highly expressed RA-generating enzyme, we compared RARE activation during the course of differentiation in WT and *Aldh1A1*$^{-/-}$ fibroblasts permanently transfected with a RARE- luciferase reporter (**Figure 4C**). Differentiation in WT fibroblasts was accompanied by RARE activation, whereas during differentiation of *Aldh1A1*$^{-/-}$ adipocytes, RARE activation was markedly reduced as compared to WT adipocytes (64% reduction at day 7). The decreased RARE activation was consistent with the absence of *Aldh1A1*, the low expression levels of other Aldh1 enzymes, and impaired differentiation that

manifested as higher expression ratio of preadipocyte marker *Pref1* to adipocyte differentiation marker *Fabp4* (**Supplementary Figure 5**). To establish a link between decreased RA generation in *Aldh1A1* deficiency and mTORC1 regulation, WT and *Aldh1A1*$^{-/-}$ adipocytes were stimulated with insulin with or without rapamycin. The insulin treatment increased p70S6K phosphorylation, which was inhibited by rapamycin in WT adipocytes, but in *Aldh1A1*$^{-/-}$ adipocytes insulin and rapamycin did not have influence the levels of phosphorylated p70S6K (**Figure 4D**). In differentiated 3T3-L1 adipocytes, both rapamycin and Rald suppressed insulin-mediated phosphorylation of p70S6K (**Supplementary Figure 5B**). RA supports p70S6K phosphorylation in WT and 3T3-L1 adipocytes, while rapamycin abolished RA-mediated p70S6K phosphorylation (**Supplementary Figure 4C**).

In our RARE assay, *Aldh1A1* deficiency manifested as reduced RA generation in visceral fat from female, but not male mice in vivo (**Figure 2E**). Consistent with the changes in RA metabolism, we found significantly reduced p70S6K phosphorylation only in *Aldh1A1*$^{-/-}$ females (**Figure 4E**). Of note, these differences were seen in starved (18h) mice without insulin treatment, and thus represent 'basal' differences in mTORC1 activation. Previous genetic studies in mice with disrupted mTORC1 pathways highlighted increased thermogenesis as a key mechanism responsible for the resistance to diet-induced obesity seen in these mice (14, 36). We compared thermogenesis markers, such as uncoupling protein-1 (Ucp1) between female and male *Aldh1A1*$^{-/-}$ mice (**Figure 4F**). In agreement with mTORC1 suppression in *Aldh1A1*$^{-/-}$ females, markedly higher *Ucp1* mRNA expression and protein levels were observed in visceral fat from *Aldh1A1*$^{-/-}$ female compared to *Aldh1A1*$^{-/-}$ male mice. Consequently, body temperature was increased only in *Aldh1A1*$^{-/-}$ females compared to all other groups.

<u>Aldh1 enzymes regulate visceral fat formation in ovariectomized mice</u>

The female-specific expression of *Aldh1* enzymes rises the question of whether vitamin A metabolism influences visceral fat formation induced by estrogen deficiency. A causal relationship between *Aldh1A1*

and female-specific visceral obesity was established in sham-operated and ovariectomized WT and *Aldh1A1*$^{-/-}$ mice on regular chow. Ovariectomy did not alter the expression of Rald-producing enzymes in visceral fat, with the exception of decreased *Adh4* in the WT sham group compared to all other groups (**Figure 5A,** left panel). In contrast, RA-producing enzymes in visceral fat showed altered expression from ovariectomy. Ovariectomized WT females expressed elevated *Aldh1A1* and significantly increased *Aldh1A3* mRNA levels compared to WT sham-operated females (**Figure 5A,** right panel). Accordingly, expression of *Cyp26A1* was higher in ovariectomized than in sham WT females (**Figure 5A**, insert). *Aldh1A1* deficiency significantly decreased expression of both *Aldh1A2* and *Aldh1A3* in sham-operated *Aldh1A1*$^{-/-}$ compared to WT females. Ovariectomized *Aldh1A1*$^{-/-}$ females also expressed less *Aldh1A3* than ovariectomized WT mice.

As in the diet-induced obesity model, the deficiency in RA-generating enzymes in *Aldh1A1*$^{-/-}$ ovariectomized females resulted in decreased phosphorylation of p70S6K and 4Ebp1 in *Aldh1A1*$^{-/-}$ compared to WT ovariectomized mice (**Figure 5B**). In consonance with the suppression of these mTORC1 downstream targets, Atgl had increased protein levels, but not mRNA expression levels in the visceral fat of *Aldh1A1*$^{-/-}$ versus WT ovariectomized mice (**Figure 5C**). The limited mTORC1 suppression was evinced in the reduced fat formation in diet-induced obesity models. In fact, whereas WT females gained weight following ovariectomy as expected (**Supplementary Figure 6A**), ovariectomized *Aldh1A1*$^{-/-}$ females had similar weight gain to sham-operated females. Food intake was also lower in ovariectomized *Aldh1A1*$^{-/-}$ females (**Supplementary Figure 6B**). These differences in weight gain depend in part on changes in visceral fat mass. The ovariectomized WT females had significantly increased visceral fat mass compared to WT sham females (240%), whereas visceral fat mass in ovariectomized *Aldh1A1*$^{-/-}$ females remained identical to sham-operated females (**Figure 5D**). MRI scans revealed that *Aldh1A1*$^{-/-}$ females retained basal visceral fat, but did not develop visceral fat after ovariectomy (**Figure 5E**).

Visceral fat in women expresses *Aldh1A1*

To gain insight into relevance of Aldh1A1 for visceral fat biology in women, we analyzed expression of *Aldh1* enzymes in non-differentiated (nD) and differentiated primary visceral preadipocytes (**Figure 6A**). Differentiation of visceral preadipocytes was accompanied by markedly increased expression of *Aldh1A1* (238%), which was significantly higher than the increase in *Aldh1A3* expression (153%). In non-differentiated (nD) adipocytes, *Aldh1A3* expression was higher than that of *Aldh1a1* (3.8E-6±2.9E-6 vs. 1.6E-7±2.5E-7 AU). *Aldh1A2* expression was 10-times lower than *Aldh1A1* expression and was further decreased during adipogenesis (57% compared to nD).

We also analyzed visceral fat isolated from three overweight premenopausal women (**Figure 6B**). In women, *Aldh1A1* mRNA expression was the most abundant among Aldh1 enzymes. *Aldh1A1* expression was significantly higher than that of *Aldh1A3*. Thus, in both female humans and rodents, *Aldh1A1* is an important enzyme in visceral fat whose expression is induced during adipogenesis.

DISCUSSION

The etiology of visceral obesity is not fully understood, although it is clear that sex hormones govern fat distribution between subcutaneous and visceral depots (5). Here we show that the Aldh1A1 enzyme that generates RA is essential for the formation of visceral fat in female mice. Our conclusion is based on the comparison of WT and *Aldh1A1*$^{-/-}$ responses to a high-fat diet and to estrogen deprivation induced by ovariectomy. *Aldh1A1* deficiency was sufficient to nearly prevent visceral fat formation in these two models (Figures 1, 5). This response was sex-specific, as *Aldh1A1*$^{-/-}$ and WT males developed similar amounts of visceral fat mass on a high-fat diet. Our finding in the *Aldh1A1*$^{-/-}$ mouse model appears relevant to humans, since *Aldh1A1* was abundantly expressed in visceral fat of women in vivo and differentiated adipocytes in vitro (Figure 6). Visceral obesity in humans increases their risks of premature death related to the development of type 2 diabetes, certain cancers, and cardiovascular disease (4, 5). Importantly, the changes in visceral fat formation in these mouse groups corresponded to changes in glucose tolerance; e.g., *Aldh1A1*$^{-/-}$ females were maintaining normal glucose levels compared to the other groups. Thus, the *Aldh1A1*$^{-/-}$ model is potentially useful to study sex-specific metabolic responses associated with visceral obesity.

The mechanism by which Aldh1a1 influences sex-specific differences in visceral fat depends on the RA that is generated by all Aldh1 enzymes. Aldh1A1 expression was similar in WT male and female mice (Figure 2). In contrast, *Aldh1A2* and *Aldh1A3*, was lower in WT females than in WT males, leaving Aldh1A1 as the major enzyme for RA production in females. Aldh1A1 produces RA from Rald, and the absence of this enzyme shifts the equilibrium between Rald and RA towards increased Rald concentrations (23, 28, 37). Consequently, *Aldh1A1*$^{-/-}$ females developed deficient RA production (Figure 2E), whereas *Aldh1A1*$^{-/-}$ males maintained similar RA levels to WT mice. Studies in RARE-reporter-containing adipocytes further highlight the impact of Aldh1A1 on RA production, which was decreased by 70% in *Aldh1A1*$^{-/-}$ compared to WT adipocytes (Figure 4C).

The mechanism behind suppressed *Aldh1A2* and *Aldh1A3* expression in visceral fat is yet to be defined, although our ovariectomy study demonstrated a significant increase in *Aldh1A3* expression in ovariectomized vs. sham-operated mice (Figure 5A). This suggests an estrogen/estrogen receptor-dependent mechanism for *Aldh1A3* regulation (**Schematic**), which is in line with the published reports about *Aldh1A2* and *Aldh1A3* regulation by estrogen and its nuclear receptor in other tissues (18, 19, 38). In RARE adipocyte cultures, estrogen stimulation also inhibited RARE activation in *Aldh1A1*$^{-/-}$ but not in WT adipocytes (data not shown). In the present study, we could not determine whether the sex-specific changes in RA production uniquely affect visceral adipose tissue. More probably, Aldh1A1 plays different roles in different tissues (8) and also in different fat depots. For example, in our studies, both *Aldh1A1*$^{-/-}$ males and females developed less subcutaneous fat than the respective WT mice (data not shown). This sex-independent response was likely due to the transcriptional repression of PPARγ by Rald (23, 28, 37). In visceral fat, we propose a paradigm of tandem regulation of sex-specific vitamin A metabolism by the action of sex hormones on the enzymes controlling Rald and RA production. This sex-specific production of RA can potentially take place in other tissues and during development. Future experiments need to examine whether increased RA generation accompanies visceral fat formation in women after menopause.

In *Aldh1A1*$^{-/-}$ female mice, there was an apparent discrepancy between the modest 20% decrease in RA generation (Figure 2E) and the remarkable 80% decrease in visceral fat and glucose tolerance (Figure 1) compared to other mouse groups. To prove the concept that sex-specific metabolic changes depend on diminished RA production, we injected RA and measured glucose tolerance in *Aldh1A1*$^{-/-}$ females (Figure 2F). When compared to *Aldh1A1*$^{-/-}$ females injected with vehicle, RA-injected *Aldh1A1*$^{-/-}$ female mice were significantly more glucose tolerant (Figure 2F). Since RA injection could not abolish glucose tolerance in *Aldh1A1*$^{-/-}$ females, it is plausible that glucose intolerance WT females also depends

on other mechanisms. The response to RA varies in different animal models and is difficult to compare due to diverse methods of RA administration. Recent studies showed that RA releasing pellets (RA concentration in plasma is unknown) in WT mice lead to a temporal weight loss (39). Similar weight loss was found with subcutaneous injections of RA (10-100mg/kg body weight) (40) whereas in the other studies oral administration (41) of release of RA from microspheres (6.5 ng RA/ml plasma) (42) did not influence weight in rats. Importantly, in humans one clinical manifestation of all-*trans*-RA treatment in acute promyelocytic leukemia patients is weight gain (43). Given that RA administration also causes sex-specific metabolic responses (41), more studies are needed to dissect specific pathways accounting for the differences seen with RA treatments. In our studies, administration of RA impairs glucose tolerance in *Aldh1A1*$^{-/-}$ females, suggesting that an *Aldh1A1*$^{-/-}$ phenotype resulted, partially, from deficient RA generation in these females (Figure 2F, left panel). Vice versa, the treatment with Rald somewhat improved glucose intolerance in WT females even after 300 days on a HF diet (Figure 2F, right panel). Rapid response to RA (30min) was previously reported in neurons that develop dendritic protrusions after RA activation of MAPK and mTOR-dependent translation (11).

To gain a global view of the mechanisms participating in sex-specific visceral fat growth, we performed a comparative proteomic analysis in WT and *Aldh1A1*$^{-/-}$ male and female mice (Supplementary Figure 3). Together, proteomic and mRNA expression analysis (Table1), can provide comprehensive information about changes in protein modification, protein levels, and mRNA expression, thereby highlighting mechanisms responsible for sexual dimorphism in *Aldh1A1*$^{-/-}$ visceral fat. These studies revealed that protein levels of 13 identified proteomic markers were changed in a sex-specific manner. Many differences in mRNA levels were seen between WT and *Aldh1A1*$^{-/-}$ mice, but they occurred in a sex-independent manner (Table 1). Of note, *Aldh1A1* deficiency led to the expected decrease in mRNA expression of RA- and/or glitazone-responsive leptin, vaspin, and caspase 1 (Supplementary Figure 4) (30-33). Given that glitazones activate PPARγ-dependent transcription, this expression pattern is

consistent with the transcriptional roles of RA (9) and Rald (23). These observations imply transcriptional regulation of differences in WT and *Aldh1A1*$^{-/-}$ fat formation, whereas non-genomic actions of vitamin A metabolites mediate, to some extent, the sex-specific effects in *Aldh1A1*$^{-/-}$ visceral fat.

Here, we studied the regulation of Atgl as a representative example of the sex-specific changes resulting from *Aldh1A1* deficiency. Atgl is a recently discovered critical enzyme for triglyceride lipolysis in adipose tissue and the heart (34). Atgl's link to vitamin A metabolism is examined here for the first time. Atgl mRNA expression was identical in all groups (Figure 3A). In contrast, Atgl protein levels were markedly higher in *Aldh1A1*$^{-/-}$ females than males (Figure 3B). The proteomic data underscores the translational mechanisms as a possible mediator of female-specific differences resulting from decreased RA production from Rald. Previous publications demonstrated that *Aldh1A1* deficiency decreased Rald catabolism to RA and increased Rald levels in *Aldh1A1*$^{-/-}$ adipose and other tissues (23, 28, 37). Our hypothesis that the Rald to RA ratio can directly influence translational responses was further examined in cultured adipocytes stimulated with RA or Rald. Whereas Rald increased Atgl protein levels rapidly (40 min), RA had no such effect (Figure 3C). The translation of many proteins in adipose tissue is under the control of mTORC1 kinase's phosphorylation of p70S6 kinase (35). Rapamycin acts solely through mTORC1 and is a first indicator of this pathway at work. In the presence of rapamycin, adipocytes produced increased Atgl protein (Figure 3D). To test if retinoids exert their effects through mTORC1, we performed short-term stimulation of HEK293 cells with or without Rald and RA in the presence of insulin and subsequently analyzed these cells for p70S6K phosphorylation by mTORC1. While Rald acted in a rapamycin-like fashion, RA activated p70S6K phosphorylation in HEK293 cells and in adipocytes (Figure 3E). A recent study demonstrated that similar RA activation of mTORC1 occurs in neurons and is mediated by a cytosolic RAR receptor (25). Here we suggest a specific non-genomic action of Rald.

Additional evidence that the intrinsic ratio of Rald to RA in cells regulates mTORC1 activation was demonstrated in vitro in differentiated WT and *Aldh1A1*$^{-/-}$ adipocyte cultures and in vivo in WT and *Aldh1A1*$^{-/-}$ adipose tissue. Insulin stimulation activated p70S6K phosphorylation in WT adipocytes, but failed to activate this kinase in *Aldh1A1*$^{-/-}$ adipocytes (Figure 4D and C). In *Aldh1A1*$^{-/-}$ visceral fat, RA generation was impaired in females (Figure 2E), and only females had significantly decreased p70S6K phosphorylation (Figure 4E). A decrease in mTORC1 activation in adipocytes can change multiple adipose tissue responses and glucose tolerance (14). The targeted disruption of the mTORC1 catalytic subunit, raptor, in adipose tissue renders these mice resistant to diet-induced obesity and glucose intolerance. This phenotype is a result of increased mRNA and protein levels of Ucp1, a key thermogenic protein (14), and phosphorylation of IRS1 (35). Notably, similar thermogenic changes, resistance to obesity, and insulin sensitivity also occur in *p70S6K*$^{-/-}$ mice and in WT mice treated with rapamycin (13, 36). *Aldh1A1* deficiency in mice decreases RA production and increases Rald levels only in females, resulting in sex-specific mTORC1 inhibition (Figure 4E). These effects were to some extent reversible, e.g. glucose tolerance was partially impaired with RA in *Aldh1A1*$^{-/-}$ females and Rald improved glucose intolerance in WT females (Figure 2F). In agreement with the mTORC1 mechanism of repression in *Aldh1A1*$^{-/-}$ females, all bona fide effects of mTORC1 inhibition were manifested in *Aldh1A1*$^{-/-}$ female but not male mice, including increased Ucp1 expression and protein levels (Figure 4F), increased temperature, improved glucose tolerance, and resistance to diet-induced visceral obesity (Figure 1). The sex-specific increase in thermogenic proteins alone provides a reasonable explanation for the resistance to obesity seen in *Aldh1A1*$^{-/-}$ female but not male mice. These in vivo data, combined with our previous in vitro observations, demonstrate that Rald and RA regulate mTORC1 in opposite fashions, with Rald inhibiting, and RA activating mTORC1. While the metabolic role of mTORC1 is just emerging, the role of mTORC1 in cancer and aging has been well documented (14, 35, 44). Remarkably, rapamycin treatment increased lifespan in female more than in male monkeys in the recent longevity study (44).

Thus, divergent regulation of mTORC1 by the endogenous metabolites, RA and Rald, and their converting enzymes could have wide implications in understanding tumorigenesis and aging.

While our first study is aimed at defining a relevant mechanism for visceral fat inhibition in *Aldh1A1*$^{-/-}$ mice, many emerging questions remain unanswered: What leads to mTORC1 inhibition: the deficiency in RA or the increase in Rald?; What protein in the mTORC1 signaling cascade is affected by retinoid production? The speculations could include cytosolic RAR interaction with RA proposed previously (11). RAR contains lysines in its ligand binding domain (45) ,and lysines bind aldehydes, such as Rald (46); however, this possible interaction needs to be addressed experimentally. To further establish the relevance of *Aldh1A1* deficiency on mTORC1 inhibition and the relevance of this mechanism for visceral obesity, we turned to a female-specific visceral obesity model, namely ovariectomy- induced estrogen deprivation. Ovariectomized WT mice gain weight on regular chow, thereby minimizing the impact of oxidized lipids, which could serve as a substrate for the Aldh1A1 enzyme. Ovariectomy in WT females leads to modest up-regulation of one RA-generating enzyme, *Aldh1A3*; in *Aldh1A1*$^{-/-}$ mice, however, the expression of all RA-generating enzymes was suppressed (Figure 5A). These changes in the vitamin A pathway result in significant suppression of mTORC1 downstream targets p70S6K and 4Ebp, and an increase in Atgl protein levels associated with this pathway (Figure 5B, C). Consequently, ovariectomy failed to induce visceral obesity in *Aldh1A1*$^{-/-}$ females (Figure 5D, E). Similar to the diet-induced obesity model, in the ovariectomized model, Aldh1A1 was a critical mediator of visceral obesity that proceeded at least in part by mTORC1. Given the pluripotent effects of RA and Rald (8, 10), a variety of other not yet identified mechanisms could contribute to the *Aldh1A1*$^{-/-}$ phenotype and the differences seen in diet- and ovariectomy-induced visceral fat formation. Of note, the basal levels of visceral fat that developed in WT and *Aldh1A1*$^{-/-}$ mice on a regular chow were not markedly affected by *Aldh1A1* deficiency (Figure 5E), suggesting Aldh1A1's role in adaptive responses. The necessity of Aldh1A1 in the regulation of visceral obesity in response to dietary or hormonal stress makes this gene a candidate for anti-obesity therapy.

Aldh1A1 is expressed in adipose tissue in women (Figure 6); in the future, clinical studies should clarify whether this gene can serve as a therapeutic target for visceral obesity in women.

Numerous clinical data suggest that metabolic disorders should be treated differently in men and women (3), which show the need for investigation of molecular mechanisms for sex-specific metabolic differences. Here, we demonstrate that a substantial part of visceral fat formation in females, but not males, depends on Aldh1A1.

MATERIALS AND METHODS

Reagents: We purchased reagents from Sigma-Aldrich and cell culture media from Invitrogen unless otherwise indicated; antibodies to phosphop70s6 kinase (Thr389) (p70S6K_P) were from Millipore, to total p70S6K, Atgl, and Gapdh were from Cell Signaling Technology, to β-actin and tubulin were from Abcam; infrared labeled secondary antibodies were from LI-COR. We used all-*trans* retinoid isomers. We purchased the Cignal Lenti inducible RARE reporter vector from SABiosciences.

Human subjects: mRNA was isolated from fat tissue, which was obtained from healthy women who underwent surgery as kidney donors and had given informed consent. The protocol was approved by the Mayo Clinic Institutional Review Board for Human Research. Subjects were 41 ± 2 yr of age. The subjects' mean body mass index (BMI) was 30.3± 0.4 kg/m^2 (more information in supplementary materials). Human primary preadipocytes were isolated from visceral fat as described in supplementary materials and were used for cell culture experiments.

Animal studies: Generation and characterization of *Aldh1A1*$^{-/-}$ mice, including metabolic responses to a high-fat diet, have been previously described (8, 23, 47). All experimental protocols were approved by the Institutional Animal Care and Use Committee.

I Diet-induced obesity study: Age-(8 weeks old) and sex-matched *Aldh1A1*$^{-/-}$ and WT mice (5 males, 5 females per genotype) were fed either regular chow or a high-fat diet (HF, 45% fat/kcal with standard vitamin A content, 4IU/g, D12451, Research Diets Inc., Canada) for 180 days. This study was performed two times. Third study was performed identically, but mice were fed the same HF diet for 300 days (*Aldh1A1*$^{-/-}$: 5 males and 10 females; WT: 4 males and 5 females).

II Ovariectomy study: Seven-month-old WT and *Aldh1A1*$^{-/-}$ females were ovariectomized or sham-operated (n=5 per genotype in each surgery group).

Weight and food consumption were measured weekly to monitor metabolic changes. Body composition was measured by dual-energy X-ray absorptiometry (DEXA) using a GE Lunar Corporation PIXImus2 Dexa Scanner and normalized to a quality control plot (Charles River Laboratories). MRI of the intraperitoneal area was performed as described before (48) using a T1-weighted gradient-echo sequence on mice at the end of the study. Twenty-five contiguous, 1-mm thick axial GRE slices spanning the region from the superior pole of the uppermost kidney to the caudal aspect of each mouse were obtained using a spin-echo sequence with a 256 X 256 matrix size. Visceral (perigonadal) and subcutaneous fat pads were dissected and analyzed.

Food and water intake were measured after mouse acclimation to a powdered HF diet (4 d) in metabolic cages (Ancare, Charles River Laboratories). Glucose tolerance tests (GTT) were performed in overnight fasted mice by intraperitoneal injection of a single 25% dextrose injection (0.004 ml/g body weight) using a glucometer for measurements (Accu-Chek Advantage, Roche or one Touch Ultra, LifeScan). Retinoic acid (0.1% 500nM concentration in ethanol) was injected in 1mL PBS, while 0.1% ethanol in 1mL PBS was injected to control animals 10 min prior to standard GTT.

Lipid extraction. We dissected adipose tissue (~100mg) into tubes containing 200uL RIPA buffer with 20μM EDTA under an argon atmosphere in the dark. Samples were immediately homogenized. One aliquot (20 μl) of sample homogenate was used to measure protein concentration. Another aliquot (100μL) of tissue homogenate was mixed with 100μl of PBS containing ~20μM EDTA, and, subsequently with 200μL of ethanol. More argon was added to prevent oxidation, then 4ml n-hexane was added and vortexed for 1min. The lipophilic phase was separated by centrifugation, transferred into a new argon-containing tube, and dried under nitrogen. Lipid extracts were re-suspended in absolute ethanol to have identical protein concentrations (5μg protein/50μL ethanol). This entire procedure was carried out at 4°C in the dark. RARE containing cells (see 'Transfection') were stimulated with lipid extract solution (0.1%) in DMEM medium containing 1% delipidated serum in the dark. For recovery measurements, adipose tissue homogenate was substituted with 100nM RA and underwent similar extraction.

Cell culture: Murine 3T3-L1 preadipocytes were cultured, maintained, and differentiated using standard procedures (23, 49). Preadipocyte cell lines were derived from embryos of WT (F_{WT}) and *Aldh1A1*$^{-/-}$ ($F_{Aldh1A1KO}$) as previously described (23, 49). In all preadipocyte cultures, differentiation was induced (day 0) with a standard differentiation mixture of 3-isobutyl-1-methylxanthine (0.5mM), dexamethasone (1μM), and insulin (1.7 μM) in DMEM containing 10% fetal bovine serum (FBS). For differentiation into adipocytes, cells were maintained for 7 days in DMEM medium containing 10% FBS and insulin (1.7 μM), which was replaced every 48h. To produce mature adipocytes, 3T3-L1 preadipocytes were cultured from 7 to 12 days. Stimulation was performed in serum-free medium. Retinoids were protected from light throughout incubation and stored under an argon atmosphere.

Human visceral (omental) preadipocytes were isolated from a female donor as described in Supplementary materials. Preadipocytes were differentiated as described previously (50) using plating medium without serum supplemented with 100 nM dexamethasone, 500 nM human insulin, 200 pM triiodothryonine, 0.5 μM rosiglitazone, antibiotics, and 540 μM isobutylmethylxanthine (removed after 2 days). Cells were differentiated for 21 days. Medium was changed weekly.

Protein analysis and Proteomic 2-D Fluorescence Difference Gel Electrophoresis (DIGE): We prepared tissue homogenates and cell lysates in radioimmunoprecipitation assay buffer (RIPA) containing complete protease and phosphatase inhibitors with EDTA (Hoffman-LaRoche). Protein content was measured by Bicinchoninic acid protein assay (Thermo Fisher Scientific).

Four homogenates from visceral fat each from males and females of WT and *Aldh1A1*$^{-/-}$ genotypes were precipitated with 10% trichloroacetic acid and used for DIGE (GE Healthcare) according to the manufacturer protocol (see Supplement Methods). Samples were labeled with DIGE fluor minimal-label dyes and focused on 18cm pH 4-7 Immobiline strips using an IPGphor II IEF. After SDS-PAGE, individual gels (containing one each of cy2, cy3, and cy5 images) were spot mapped using the Decyder

512 Differential image analysis module and analyzed by Decyder Biological Variation Analysis software
513 using internal standard (cy2) images. Statistical analysis between WT and *Aldh1A1*$^{-/-}$ groups in males and
514 females (P<0.05, independent t-test) was performed to identify spots with more than 1.5 fold differences
515 in abundance, and spots appeared in at least 3 of the 4 gels. We identified 176 spots in male and 167 spots
516 in female groups that were different between WT and *Aldh1A1*$^{-/-}$ mice without false discovery rate
517 correction (FDRC). Only 13 proteins that were significantly different between WT and *Aldh1A1*$^{-/-}$ mice
518 after FDRC analysis were spotted and identified. We define them as **proteomic markers** in this paper.
519 Significantly changed spots were matched between analytical gels and preparative gels, and then cored
520 from preparative gels using an Ettan workstation. We identified extracted peptides using a capillary liquid
521 chromatography system equipped with a LTQ mass spectrometer (MS) detector (CCIC MS and
522 Proteomics facility, the Ohio State University Medical Center). MS data was searched using Mascot
523 (scores of >40 were accepted). Expression of proteomic markers was further verified using Western blot
524 or TaqMan analysis of mRNA expression using visceral fat from the same mice.
525 For Western blot analyses, cell or tissue lysates were separated on 10% acrylamide gel under reducing
526 conditions. After transfer to a polyvinylidene fluoride membrane (Immobilon-P, Millipore), proteins were
527 analyzed using an Odyssey Infrared Imaging System (LI-COR).
528
529 **Histology:** We embedded adipose tissue in paraffin before hematoxylin and eosin (H&E) staining
530 followed by quantification of adipocyte size (ImageJ software).
531
532 **Analysis of mRNA**: mRNA was isolated from adipose tissue and adipocyte cultures according to
533 manufacturer's instructions (Qiagen). For semi-quantitative analysis of expression, cDNA was prepared
534 from purified mRNA and analyzed using 7900HT Fast Real-Time PCR System and TaqMan fluorogenic
535 detection system (Applied Biosystems). Validated primers were also purchased from Applied Biosystems.
536 Reference sequences, gene names, and aliases are described in **Supplementary Table 1**. Comparative

real-time PCR was performed in triplicate, including no-template controls. The mRNA expression of the genes of interest was compared to 18S expression levels. Relative expression was calculated using the comparative Ct method.

Transfection studies: We derived stably transfected 3T3L1, WT (F_{WT}), and *Aldh1A1*$^{-/-}$ ($F_{Aldh1A1KO}$) according to manufacturer instructions (SA Bioscience). Briefly, after reaching 70% confluence cells were transfected with Cignal Lenti RARE-LUC reporter suspension (25 MOI/10^4 cells) in the presence of Polybrene (Millipore) transduction reagent in serum free MEM-medium. After 3hrs, cells were supplemented with 10% heatinactivated calf serum. Stable clones were selected and derived from the single cells selected by puromycin (0.75-1.5mg/mL, Invitrogen). We measured luciferase activity using a dual-luciferase reporter assay (Promega).

Statistical analysis: Data are shown as mean±SD or mean±SE of experiments which were performed at least in triplicate. Group comparisons were performed using Mann Whitney U test unless otherwise indicated, and correlations were examined by Pearson test.

ACKNOWLEDGMENTS

We express our gratitude to the Mass Spectrometry and Proteomic Facility (MSPF), and the Nucleic Acid Shared Resource at The Ohio State University for excellent technical and intellectual support. We also thank R. J. Sessler (former member of O.Z. lab) and N. M. Kleinholz (MSPF) for the proteomic analysis as well N.E. Gleyzer for the preparation of these samples. We thank T.Tchkonia (Mayo Clinic), M. Belury (The Ohio State University), and the PIs at NICHD BIRCWH Center (K12 HD051959-01, Harvard University) for helpful discussions.

REFERENCES

1. Li C, Ford ES, McGuire LC, Mokdad AH 2007 Increasing trends in waist circumference and abdominal obesity among US adults. Obesity (Silver Spring) 15:216-224
2. Empana JP, Ducimetiere P, Charles MA, Jouven X 2004 Sagittal abdominal diameter and risk of sudden death in asymptomatic middle-aged men: the Paris Prospective Study I. Circulation 110:2781-2785
3. Canoy D, Boekholdt SM, Wareham N, Luben R, Welch A, Bingham S, Buchan I, Day N, Khaw KT 2007 Body fat distribution and risk of coronary heart disease in men and women in the European Prospective Investigation Into Cancer and Nutrition in Norfolk cohort: a population-based prospective study. Circulation 116:2933-2943
4. Zhang C, Rexrode KM, van Dam RM, Li TY, Hu FB 2008 Abdominal obesity and the risk of all-cause, cardiovascular, and cancer mortality: sixteen years of follow-up in US women. Circulation 117:1658-1667
5. Perrini S, Leonardini A, Laviola L, Giorgino F 2008 Biological specificity of visceral adipose tissue and therapeutic intervention. Arch Physiol Biochem 114:277-286
6. Pasquali R 2006 Obesity and androgens: facts and perspectives. Fertil Steril 85:1319-1340
7. Maden M 2007 Retinoic acid in the development, regeneration and maintenance of the nervous system. Nat Rev Neurosci 8:755-765
8. Duester G 2008 Retinoic acid synthesis and signaling during early organogenesis. Cell 134:921-931
9. Germain P, Chambon P, Eichele G, Evans RM, Lazar MA, Leid M, De Lera AR, Lotan R, Mangelsdorf DJ, Gronemeyer H 2006 International Union of Pharmacology. LX. Retinoic acid receptors. Pharmacol Rev 58:712-725
10. Ziouzenkova O, Plutzky J 2008 Retinoid metabolism and nuclear receptor responses: New insights into coordinated regulation of the PPAR-RXR complex. FEBS Lett 582:32-38
11. Chen N, Napoli JL 2008 All-trans-retinoic acid stimulates translation and induces spine formation in hippocampal neurons through a membrane-associated RARalpha. FASEB J 22:236-245
12. Takano A, Usui I, Haruta T, Kawahara J, Uno T, Iwata M, Kobayashi M 2001 Mammalian target of rapamycin pathway regulates insulin signaling via subcellular redistribution of insulin receptor substrate 1 and integrates nutritional signals and metabolic signals of insulin. Mol Cell Biol 21:5050-5062
13. Chang GR, Chiu YS, Wu YY, Chen WY, Liao JW, Chao TH, Mao FC 2009 Rapamycin protects against high fat diet-induced obesity in C57BL/6J mice. J Pharmacol Sci 109:496-503
14. Polak P, Cybulski N, Feige JN, Auwerx J, Ruegg MA, Hall MN 2008 Adipose-specific knockout of raptor results in lean mice with enhanced mitochondrial respiration. Cell Metab 8:399-410
15. Le Bacquer O, Petroulakis E, Paglialunga S, Poulin F, Richard D, Cianflone K, Sonenberg N 2007 Elevated sensitivity to diet-induced obesity and insulin resistance in mice lacking 4E-BP1 and 4E-BP2. J Clin Invest 117:387-396
16. MacLaren R, Cui W, Simard S, Cianflone K 2008 Influence of obesity and insulin sensitivity on insulin signaling genes in human omental and subcutaneous adipose tissue. J Lipid Res 49:308-323

17. Napoli JL 1996 Retinoic acid biosynthesis and metabolism. FASEB J 10:993-1001
18. Li XH, Kakkad B, Ong DE 2004 Estrogen directly induces expression of retinoic acid biosynthetic enzymes, compartmentalized between the epithelium and underlying stromal cells in rat uterus. Endocrinology 145:4756-4762
19. Wang X, Sperkova Z, Napoli JL 2001 Analysis of mouse retinal dehydrogenase type 2 promoter and expression. Genomics 74:245-250
20. Trasino SE, Harrison EH, Wang TT 2007 Androgen regulation of aldehyde dehydrogenase 1A3 (ALDH1A3) in the androgen-responsive human prostate cancer cell line LNCaP. Exp Biol Med (Maywood) 232:762-771
21. Schwarz EJ, Reginato MJ, Shao D, Krakow SL, Lazar MA 1997 Retinoic acid blocks adipogenesis by inhibiting C/EBPbeta-mediated transcription. Mol Cell Biol 17:1552-1561
22. Bonet ML, Ribot J, Felipe F, Palou A 2003 Vitamin A and the regulation of fat reserves. Cell Mol Life Sci 60:1311-1321
23. Ziouzenkova O, Orasanu G, Sharlach M, Akiyama TE, Berger JP, Viereck J, Hamilton JA, Tang G, Dolnikowski GG, Vogel S, Duester G, Plutzky J 2007 Retinaldehyde represses adipogenesis and diet-induced obesity. Nat Med 13:695-702
24. Noy N 2007 Ligand specificity of nuclear hormone receptors: sifting through promiscuity. Biochemistry 46:13461-13467
25. Zhang M, Hu P, Krois CR, Kane MA, Napoli JL 2007 Altered vitamin A homeostasis and increased size and adiposity in the rdh1-null mouse. FASEB J 21:2886-2896
26. Hessel S, Eichinger A, Isken A, Amengual J, Hunzelmann S, Hoeller U, Elste V, Hunziker W, Goralczyk R, Oberhauser V, von Lintig J, Wyss A 2007 CMO1 Deficiency Abolishes Vitamin A Production from beta-Carotene and Alters Lipid Metabolism in Mice. J Biol Chem 282:33553-33561
27. Schupp M, Lefterova MI, Janke J, Leitner K, Cristancho AG, Mullican SE, Qatanani M, Szwergold N, Steger DJ, Curtin JC, Kim RJ, Suh M, Albert MR, Engeli S, Gudas LJ, Lazar MA 2009 Retinol saturase promotes adipogenesis and is downregulated in obesity. Proc Natl Acad Sci U S A 106:1105-1110
28. Molotkov A, Duester G 2003 Genetic evidence that retinaldehyde dehydrogenase Raldh1 (Aldh1a1) functions downstream of alcohol dehydrogenase Adh1 in metabolism of retinol to retinoic acid. J Biol Chem 278:36085-36090
29. Repa JJ, Hanson KK, Clagett-Dame M 1993 All-trans-retinol is a ligand for the retinoic acid receptors. Proc Natl Acad Sci U S A 90:7293-7297
30. Kim JY, Tillison K, Lee JH, Rearick DA, Smas CM 2006 The adipose tissue triglyceride lipase ATGL/PNPLA2 is downregulated by insulin and TNF-alpha in 3T3-L1 adipocytes and is a target for transactivation by PPARgamma. Am J Physiol Endocrinol Metab 291:E115-127
31. Hida K, Wada J, Eguchi J, Zhang H, Baba M, Seida A, Hashimoto I, Okada T, Yasuhara A, Nakatsuka A, Shikata K, Hourai S, Futami J, Watanabe E, Matsuki Y, Hiramatsu R, Akagi S, Makino H, Kanwar YS 2005 Visceral adipose tissue-derived serine protease inhibitor: a unique insulin-sensitizing adipocytokine in obesity. Proc Natl Acad Sci U S A 102:10610-10615
32. Wang HN, Wang YR, Liu GQ, Liu Z, Wu PX, Wei XL, Hong TP 2008 Inhibition of hepatic interleukin-18 production by rosiglitazone in a rat model of nonalcoholic fatty liver disease. World J Gastroenterol 14:7240-7246

33. Arany I, Ember IA, Tyring SK 2003 All-trans-retinoic acid activates caspase-1 in a dose-dependent manner in cervical squamous carcinoma cells. Anticancer Res 23:471-473
34. Haemmerle G, Lass A, Zimmermann R, Gorkiewicz G, Meyer C, Rozman J, Heldmaier G, Maier R, Theussl C, Eder S, Kratky D, Wagner EF, Klingenspor M, Hoefler G, Zechner R 2006 Defective lipolysis and altered energy metabolism in mice lacking adipose triglyceride lipase. Science 312:734-737
35. Corradetti MN, Guan KL 2006 Upstream of the mammalian target of rapamycin: do all roads pass through mTOR? Oncogene 25:6347-6360
36. Um SH, Frigerio F, Watanabe M, Picard F, Joaquin M, Sticker M, Fumagalli S, Allegrini PR, Kozma SC, Auwerx J, Thomas G 2004 Absence of S6K1 protects against age- and diet-induced obesity while enhancing insulin sensitivity. Nature 431:200-205
37. Mic FA, Molotkov A, Benbrook DM, Duester G 2003 Retinoid activation of retinoic acid receptor but not retinoid X receptor is sufficient to rescue lethal defect in retinoic acid synthesis. Proc Natl Acad Sci U S A 100:7135-7140
38. Fujiwara K, Kikuchi M, Horiguchi K, Kusumoto K, Kouki T, Kawanishi K, Yashiro T 2009 Estrogen Receptor Alpha Regulates Retinaldehyde Dehydrogenase 1 Expression in Rat Anterior Pituitary Cells. Endocr J
39. Berry DC, Noy N 2009 All-trans-retinoic acid represses obesity and insulin resistance by activating both peroxisome proliferation-activated receptor beta/delta and retinoic acid receptor. Mol Cell Biol 29:3286-3296
40. Mercader J, Ribot J, Murano I, Felipe F, Cinti S, Bonet ML, Palou A 2006 Remodeling of white adipose tissue after retinoic acid administration in mice. Endocrinology 147:5325-5332
41. Rodriguez Rodriguez MS 1992 [The percutaneous catheter: the solution]. Rev Enferm 15:73-76
42. Choi Y, Kim SY, Park K, Yang J, Cho KJ, Kwon HJ, Byun Y 2006 Chemopreventive efficacy of all-trans-retinoic acid in biodegradable microspheres against epithelial cancers: results in a 4-nitroquinoline 1-oxide-induced oral carcinogenesis model. Int J Pharm 320:45-52
43. De Botton S, Dombret H, Sanz M, Miguel JS, Caillot D, Zittoun R, Gardembas M, Stamatoulas A, Conde E, Guerci A, Gardin C, Geiser K, Makhoul DC, Reman O, de la Serna J, Lefrere F, Chomienne C, Chastang C, Degos L, Fenaux P 1998 Incidence, clinical features, and outcome of all trans-retinoic acid syndrome in 413 cases of newly diagnosed acute promyelocytic leukemia. The European APL Group. Blood 92:2712-2718
44. Harrison DE, Strong R, Sharp ZD, Nelson JF, Astle CM, Flurkey K, Nadon NL, Wilkinson JE, Frenkel K, Carter CS, Pahor M, Javors MA, Fernandez E, Miller RA 2009 Rapamycin fed late in life extends lifespan in genetically heterogeneous mice. Nature 460:392-395
45. Huq MD, Tsai NP, Khan SA, Wei LN 2007 Lysine trimethylation of retinoic acid receptor-alpha: a novel means to regulate receptor function. Mol Cell Proteomics 6:677-688
46. Maiti TK, Engelhard M, Sheves M 2009 Retinal-protein interactions in halorhodopsin from Natronomonas pharaonis: binding and retinal thermal isomerization catalysis. J Mol Biol 394:472-484

47. Fan X, Molotkov A, Manabe S, Donmoyer CM, Deltour L, Foglio MH, Cuenca AE, Blaner WS, Lipton SA, Duester G 2003 Targeted disruption of Aldh1a1 (Raldh1) provides evidence for a complex mechanism of retinoic acid synthesis in the developing retina. Mol Cell Biol 23:4637-4648
48. Sun Q, Yue P, Deiuliis JA, Lumeng CN, Kampfrath T, Mikolaj MB, Cai Y, Ostrowski MC, Lu B, Parthasarathy S, Brook RD, Moffatt-Bruce SD, Chen LC, Rajagopalan S 2009 Ambient air pollution exaggerates adipose inflammation and insulin resistance in a mouse model of diet-induced obesity. Circulation 119:538-546
49. Green H, Meuth M 1974 An established pre-adipose cell line and its differentiation in culture. Cell 3:127-133
50. Tchkonia T, Tchoukalova YD, Giorgadze N, Pirtskhalava T, Karagiannides I, Forse RA, Koo A, Stevenson M, Chinnappan D, Cartwright A, Jensen MD, Kirkland JL 2005 Abundance of two human preadipocyte subtypes with distinct capacities for replication, adipogenesis, and apoptosis varies among fat depots. Am J Physiol Endocrinol Metab 288:E267-277
51. Pares X, Farres J, Kedishvili N, Duester G 2008 Medium- and short-chain dehydrogenase/reductase gene and protein families : Medium-chain and short-chain dehydrogenases/reductases in retinoid metabolism. Cell Mol Life Sci 65:3936-3949

Table 1. Proteomic and semi-quantitative expression analysis (QPCR) of visceral fat from WT and *Aldh1A1*$^{-/-}$ male and female mice

Difference in protein levels of proteomic markers measured in two groups: 1) male WT and *Aldh1A1*$^{-/-}$ mice and 2) female WT and *Aldh1A1*$^{-/-}$ mice using Proteomic 2-D Fluorescence Difference Gel Electrophoresis (DIGE) analysis (five left columns). An example of DIGE gels overlying labeled proteins in WT/KO male and female groups are shown in Supplementary Figure 3. Average ratio shows fold difference between genotypes. *T*-test (n=4). TaqMan analyses of mRNA expression of these proteins isolated from visceral fat of same animals in separate groups of 1) WT males; 2) WT males; 3) KO males; 4) KO females (four right columns), Mann-Whitney U test (n=5).

TABLE. 1

		Protein, DIGE comparative proteomic analysis				mRNA, QPCR			
		DIGE: Group 1		DIGE: Group 2		PCR Group 1	PCR Group 2	PCR Group 3	PCR Group 4
Protein name Mus musculus	Mowse score	GEL: MALES WTm vs KO m Fold	*P*	GEL: FEMALES WTf vs KOf Fold	*P*	WT vs KO (male) *P*	WT vs KO (female) *P*	Sex specific (WT) *P*	Sex specific (KO) *P*
Group 1. Significant in both groups in proteomic analysis									
Peroxiredoxin-6 (Prdx6)	703	9.47	0.008	6.28	0.002	n.s.	n.s.	n.s.	n.s.
Glyoxalase domain-containing protein 4 (Glod4)	181	5.26	0.003	5.26	0.008	n.s.	0.033	n.s.	n.s.
3'(2'),5'-bisphosphate nucleotidase 1 (Bpnt1)	693	2.56	0.037	2.82	0.005	n.s.	n.s.	n.s.	n.s.
Group 2. Significant in male group in proteomic analysis									
Glia maturation factor beta (GMFbeta)	125	9.85	0.008	8.01	n.s.	n.s.	n.s.	n.s.	n.s.
Serine (or cysteine) peptidase inhibitor, clade A, member 3A (Serpina3a)	1181	5.43	0.047	2.12	n.s.	n.s.	n.s.	n.s.	n.s.
Triacylglycerol hydrolase (Tgh, Carboxylesterase 3)	200	2.23	0.021	2.43	n.s.	n.s.	0.000	n.s.	n.s.
Nidogen-1 precursor (Nid1)	496	1.57	0.037	-1.04	n.s.	n.s.	n.s.	n.s.	n.s.
Group 3. Significant in female group in proteomic analysis									
Adipose-specific triacylglycelol lipase (Atgl)	384	2.03	n.s.	1.57	0.05	n.s.	n.s.	n.s.	n.s.
2-oxoisovalerate dehydrogenase subunit beta,(Bckdh)	237	1.54	n.s.	2.03	0.038	0.001	0.000	n.s.	n.s.
Lymphocyte cytosolic protein-1 (Lcp1, L-plastin)	995	-3.39	n.s.	-2.8	0.054	0.010	0.031	n.s.	n.s.
Carnosinase-2 (Cytosolic non-specific dipeptidase, Cndp2)	1190	-1.94	n.s.	-1.72	0.05	0.008	0.010	0.046	n.s.
Charged multivesicular body protein 5 (Chmp5)	60	-1.5	n.s.	-1.58	0.013	n.s.	n.s.	n.s.	n.s.
Caspase-1 precursor (Casp1)	470	-1.14	n.s.	-1.54	0.000	0.001	0.040	0.049	n.s.

FIGURE LEGENDS

Figure 1. Sexual dimorphism in visceral fat formation and glucose tolerance of WT and *Aldh1A1*$^{-/-}$ mice on a high-fat diet

(A) Whole body weight are shown in WT male (n=18) and female (n=17) mice on regular chow; in WT male (n=8) and female (n=9) mice on a high-fat diet (HF) for 180 days; in *Aldh1A1*$^{-/-}$ males (n=18) on regular, and (n=9, 180d and n=5, 300d) on HF and females (n=23) on regular, and (n=11;180d and n=7; 300d) on HF. 300 days of diet did not significantly increase weight in WT mice (bars are not shown, 62.6±4.2 males, 52.5±8.9 females). *, P<0.05 differences between genotypes; S, P<0.05 differences between sexes within one genotype. All Mann-Whitney U test. All data are shown as mean±SD.

(B) Water and food consumption measured in metabolic cages in mice after HF feeding for 180 days (WT (all n=5); *Aldh1A1*$^{-/-}$ males (n=5) and females, n=5). Data are shown as mean±SD.
Food consumption was measured every week; it did not differ significantly between groups throughout HF feeding (data not shown).

(C) White fat (inguinal and visceral (perigonadal)) weight in WT male and female (all, n=5) as well as in *Aldh1A1*$^{-/-}$ male and female (both, n=4) after 180 and 300 days (KO: male n=5, female n=7) on the HF diet. White fat mass in WT mice after 300d on HF diet was similar to those after 180d (4548.4±2341.9 males, 9544.8±2135.7 females). DEXA measurements of fat (%) show similar results (Supplementary Figure 1A). Data are shown as mean±SD. *, P<0.05 differences between genotypes; S, P<0.05 differences between sexes within one genotype.

(D) Visceral fat weight in same groups of animals as in (C). Visceral fat mass in WT was after 300d on HF diet similar to those after 180d (3032.5±2307.1 males, 5861.3±1767.6 females). Inserts shows representative visceral fat pads from each animal group (180d on HF diet). Mean±SD. *, P<0.05

differences between genotypes; S, P<0.05 differences between sexes within one genotype. Individual differences in visceral fat of *Aldh1A1*$^{-/-}$ male and female mice are shown in Supplementary Figure 1B.

(E) Adipocyte size was calculated based on H&E sections of visceral fat from WT and *Aldh1A1*$^{-/-}$ mice. Representative sections are shown in an insert. *, P<0.05 (n=3, mean±SD).

(F) Glucose tolerance test in WT (open symbols, dashed lines) and *Aldh1A1*$^{-/-}$ (black symbols, solid lines) males (triangles) and females (circles) on a high-fat diet (all n=4, all animals were 180 days on HF diet from study described in A-E). *, P<0.05 differences between genotypes; S, P<0.05 differences between sexes within one genotype. All data are shown as mean±SD.

Figure 2. RA generation in visceral fat of WT and *Aldh1A1*$^{-/-}$ mice is sex-specific and influences glucose tolerance

(A) Schematics of the major enzymes participating in vitamin A metabolism. Rald is generated from retinol by alcohol dehydrogenases (Adh1, Adh3, and Adh4) and retinol dehydrogenases (Rdh1 and Rdh10) that are members of short-chain dehydrogenase/reductase (Sdr) family. Other 15 Sdr members of this family have reduced activity towards all-*trans* retinol isomers and are not studied here (reviewed in (51)). RA is produced solely from Rald by the cytosolic aldehyde dehydrogenase-1 family of enzymes (Aldh1A1, Aldh1A2, and Aldh1A3). This family is also known and retinaldehyde dehydrogenases family Raldh1, Raldh2, and Raldh3). Excess RA is oxidized by Cyp26A1 and, primarily, by Cyp26B1.

(B) Relative expression of Rald-generating (left panel), RA-generating (right panel), and (C) RA-catabolizing enzymes in visceral fat isolated from WT male (n=5), WT female (n=4), and *Aldh1A1*$^{-/-}$ male and female mice (both n=4) on a high-fat diet. All data are shown as mean±SE.

(D) Luciferase reporter assays with RARE in an *Aldh1A1*$^{-/-}$ fibroblast cell line stimulated with RA (open circles) or Rald (closed circles). All data are shown as mean±SD.

(E) RARE reporter assay using lipid extracts from visceral fat of WT and *Aldh1A1*$^{-/-}$ male and female mice on a high-fat diet (mean±SE, all n=5). *, P<0.025, Kendall's W test.

(F) Left panel : Glucose tolerance test (GTT) in WT female mice with and without Rald (all on HF for 390 days). Rald (1μM/1 mL PBS) or vehicle (veh, 0.01% ethanol in 1mLPBS) were injected intraperitonelly, then with GTT test was performed. *, P<0.05 differences between vehicle and Rald treatments. The weight of WT female mice (mean±SD, n=4) in 'veh' and 'Rald' group was 52.9±8.2 and 53.1±6.7, respectively.

Right panel: Glucose tolerance test (GTT) in WT (white circles) and *Aldh1A1*$^{-/-}$ (black circles) female mice with (solid line) and without RA (dashed line). All mice were on HF diet for ~300days. The weight of WT female mice (mean±SD, n=4, both 'veh' and 'RA' groups) was 44.0±4.6; in *Aldh1A1*$^{-/-}$ female mice (mean±SD, n=3, both 'veh' and 'RA' groups) was 26.9±2.6. RA (500nM/1 mL PBS) or vehicle (veh, 0.01% ethanol in 1mL PBS) were injected intraperitonelly, after 10minutes GTT test was performed. *, *P*<0.05 differences between vehicle and RA treatments in *Aldh1A1*$^{-/-}$ female mice; # P<0.05 differences between WT and *Aldh1A1*$^{-/-}$ groups, Mann-Whitney U test.

Figure 3. Disparate effects of Rald and RA in the regulation of Atgl and the mTORC1 downstream target p70S6K

(A) *Atgl* mRNA expression measured by TaqMan and (B) protein levels measured by western blot were analyzed in visceral fat from WT and *Aldh1A1*$^{-/-}$ male and female mice (all mean±SD, n=4) on a high-fat diet. Insert shows Atgl protein levels in 3 animals from each group.

(C) Atgl levels in differentiated (8d) 3T3-L1 fibroblasts measured by western blot. Cells were stimulated for 45min with retinol (ROL), RA, and Rald (all 100nM) in 100nM insulin/20%FBS medium. Atgl levels were normalized to tubulin. Data are shown as a percent of vehicle control. Insert on the right shows a representative example of a western blot. *, difference between control (Veh) and Rald-stimulated cells; #, difference between Rald- and RA-stimulated cells, both $P<0.05$ (mean±SE, n=3).

(D) Atgl levels in differentiated (8d) 3T3-L1 fibroblasts that were stimulated with indicated concentrations of rapamycin for 70min.

(E) Phosphorylated (S6K_P, gray bars) and non-phosphorylated p70S6 (white bars) kinase levels in HEK293 cells measured by western blot. Cells were deprived from serum for 18h then stimulated with 100nM insulin/20%FBS (ins, 30min) with or without rapamycin (rapa), RA, and Rald (all 100nM, added 10min after insulin). *, $P<0.05$ (n=3, mean±SD) (inserts shows a western blot example, S6K_P antibodies (Cell Signaling) typically recognize two bands in these cells).

Figure 4. *Aldh1a1* deficiency decreases RA generation and suppresses mTOR/p70S6K in vitro and in vivo

The expression of (A) Rald-generating and (B) RA-generating enzymes in non-differentiated (Non-D) and differentiated 3T3-L1 adipocytes. TaqMan expression data were normalized using 18S as an endogenous control. Relative expression was calculated based on the comparative Ct method. *, $P<0.05$ (n=3, mean±SD).

(C) RARE-WT and RARE-*Aldh1A1*$^{-/-}$ fibroblast lines were differentiated with a standard differentiation mix and measured for luciferase activity at different days of differentiation. Data were normalized to RARE activity seen in non-differentiated cells RARE-WT and RARE-*Aldh1A1*$^{-/-}$ fibroblast (nonD). *,

826 difference between RARE activity in non-differentiated (day 0) and differentiated adipocytes; #,
827 difference between adipocytes of different genotypes, both $P<0.05$ (n=3, mean±SD).
828
829 (D) Phosphorylated (S6K_P) and total protein levels of p70S6 kinase (S6K) were measured in WT(F_{WT})
830 and *Aldh1A1*$^{-/-}$ ($F_{Aldh1A1KO}$) differentiated fibroblasts (8d) stimulated with 100nM insulin/20%FBS with or
831 without rapamycin (100nM) for 30min using western blotting. A representative example is shown in the
832 insert. Protein levels were quantified and normalized to tubulin levels. *, $P<0.05$ (n=3, mean±SD)
833 difference compared to insulin-stimulated F_{WT}.
834
835 (E) Western blot analysis of S6K_P (left panel & insert of a western blot in two animals from each
836 group), and p70S6 kinase (left panel & insert) levels in visceral fat from WT and *Aldh1A1*$^{-/-}$ male and
837 female mice (all n=4, mean±SD) on a high-fat diet. Protein levels were normalized to Gapdh or tubulin
838 for quantification. *, P<0.05 differences between genotypes; S, P<0.05 differences between sexes within
839 one genotype. S6K_P antibody recognizes protein in insulin-stimulated control cell lysates.
840
841 (F, left panel) *Ucp1* mRNA expression measured by TaqMan and (F, middle panel) protein levels
842 measured by western blot were analyzed in the same visceral fat from WT and *Aldh1A1*$^{-/-}$ male and
843 female mice as in (E). Insert shows a representative western blot from 2 animals from each group. BF-
844 brown fat control lysates.
845 (F, right panel) Rectal body temperature was measured in animals from the same study (n=5, mean±SD).
846 *, $P<0.05$ differences between genotypes; S, P<0.05 differences between sexes within one genotype.
847
848 **Figure 5. *Aldh1A1* deficiency decreases expression of RA-generating enzymes, suppresses**
849 **mTORC1, and prevents visceral fat formation induced by ovariectomy**

(A, left panel, mean±SD) Relative expression of Rald-generating, RA-generating (A, right panel, mean±SE), and *Cyp26A1* (A, insert, mean±SD) enzymes was measured in visceral fat isolated from sham-operated (n=5) and ovariectomized (OVX, n=4) WT and *Aldh1A1*$^{-/-}$ female mice on regular chow. #, P<0.05 differences between sham and ovariectomized; *, differences between ovariectomized WT and *Aldh1A1*$^{-/-}$ mice.

(B) Western blot analysis of S6K_P and p70S6 kinase, 4Ebp1_P and total 4Ebp1, and (C, left panel) Atgl levels in WT and *Aldh1A1*$^{-/-}$ sham and ovariectomized female mice (all n=4, mean±SE). Insert shows a representative western blot in two ovariectomized WT and *Aldh1A1*$^{-/-}$ mice. Protein levels were normalized to β-actin. (C, right panel) Relative expression of *Atgl* in these mouse groups was normalized by 18S.

(D) Weight of visceral fat pads and (E) cross-sectional MRI images in sham-operated (n=5) and ovariectomized (OVX, n=4) WT and *Aldh1A1*$^{-/-}$ female mice on regular chow. K, kidney; Vis, visceral fat; #, P<0.05 differences between sham and ovariectomized; *, differences between ovariectomized WT and *Aldh1A1*$^{-/-}$ mice. Data are shown as mean±SE.

Figure 6. Prevailing expression of *Aldh1A1* in the course of visceral adipogenesis and in visceral fat in women

(A) Relative changes in mRNA expression of Aldh1 enzymes in differentiated visceral (om, omental) adipocytes (21 d) compared to expression levels of each enzyme (100%) in non-differentiated preadipocytes (#, P<0.01 Mann- Whitney U test, mean±SD, n=3). The expression levels in non-differentiated preadipocytes were 1.6E-7±2.5E-8 (*Aldh1A1*), 1.4E-8±3.8E-9 (*Aldh1A2*), and 3.8E-6±2.9E-7 (*Aldh1A3*).

(B) mRNA expression (TaqMan) of *Aldh1* enzymes in visceral adipose tissue isolated from three women. Relative expression of *Aldh1* (mean±SD) in these donors was normalized by 18S using ΔCt method. #, P<0.01, differences between expression of Aldh1A1 and other Aldh1 enzymes.

Schematic 1. Proposed model for regulation of visceral obesity in females: simultaneous action of diet and estrogen regulates the expression of the Aldh1 family of enzymes. Generated Rald or RA regulates mTOR and influences translation of specific proteins including Atgl and Ucp1. The resulting changes in thermogenesis, lipolysis, and other aspects of adipocyte metabolism determine female susceptibility to visceral fat formation.

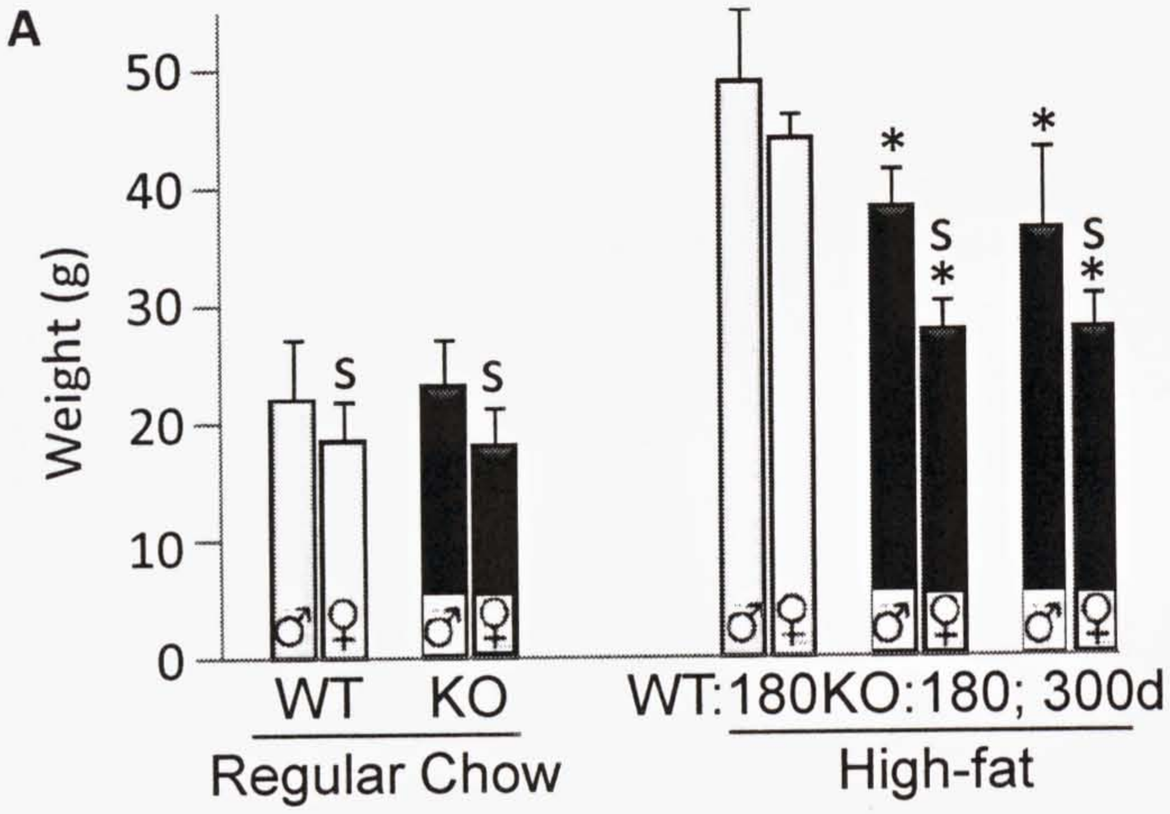

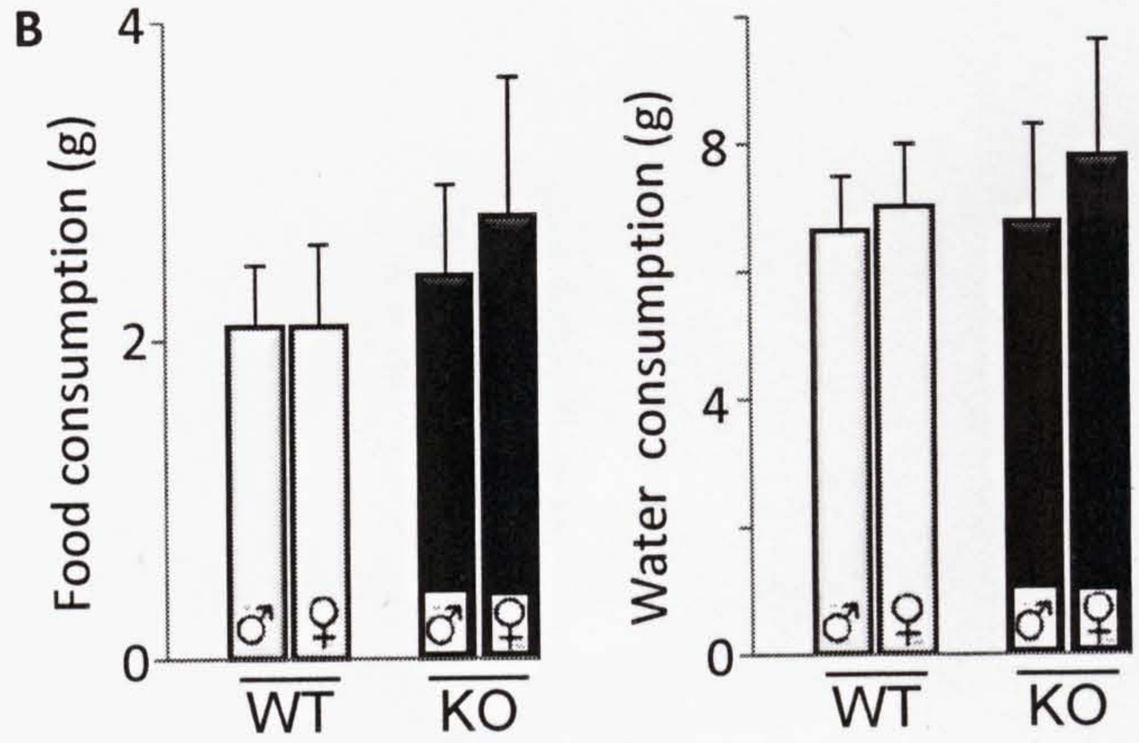

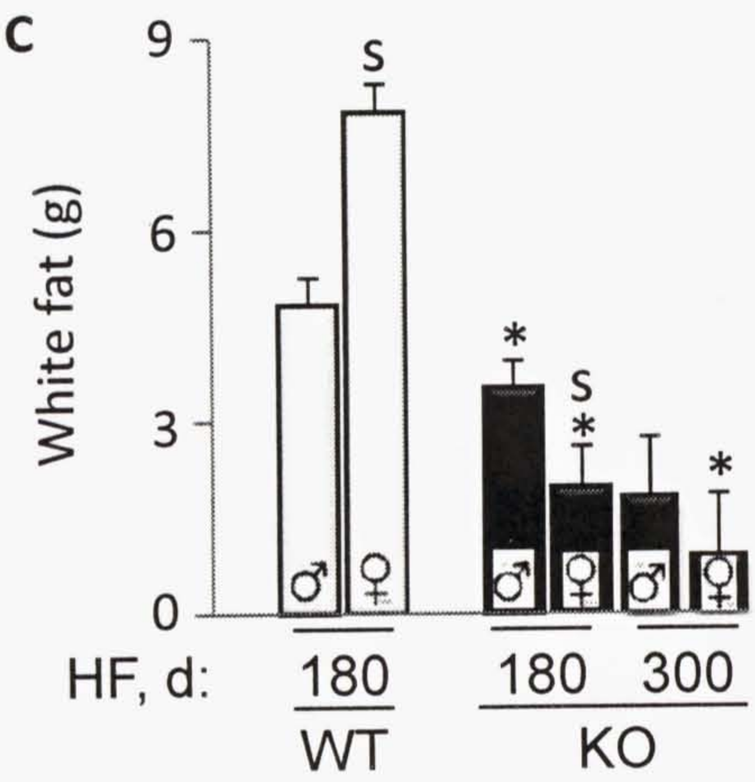

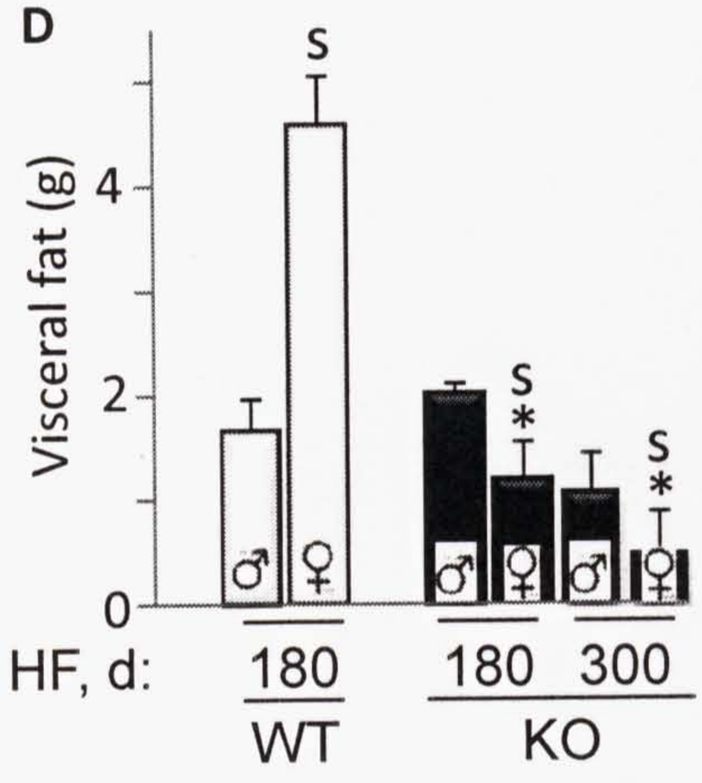

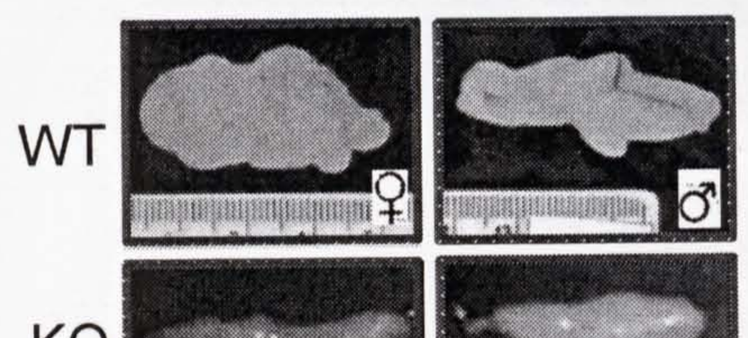

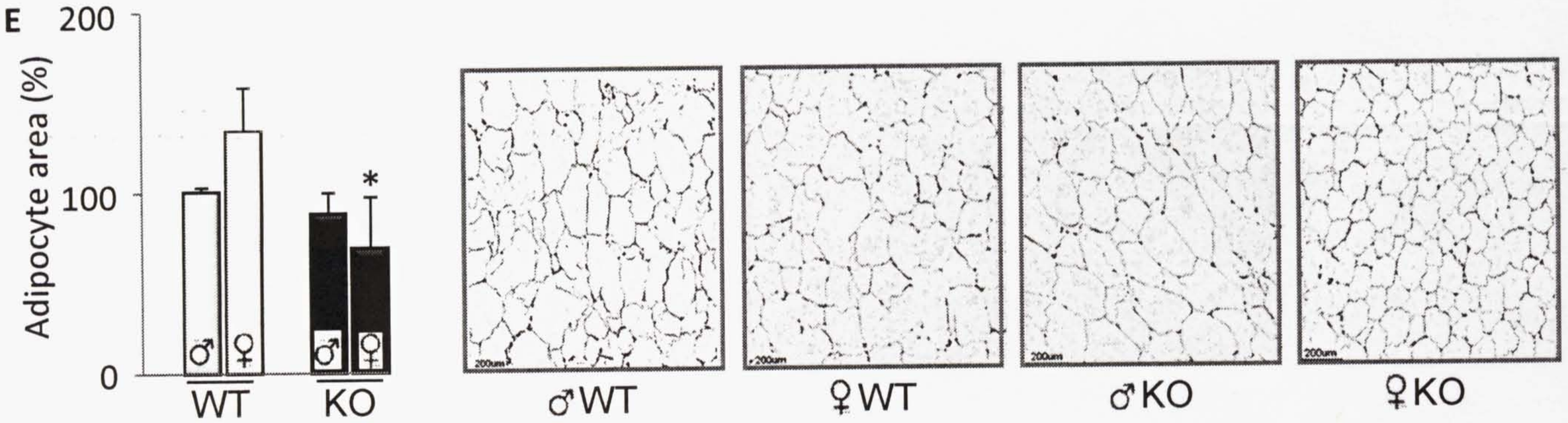

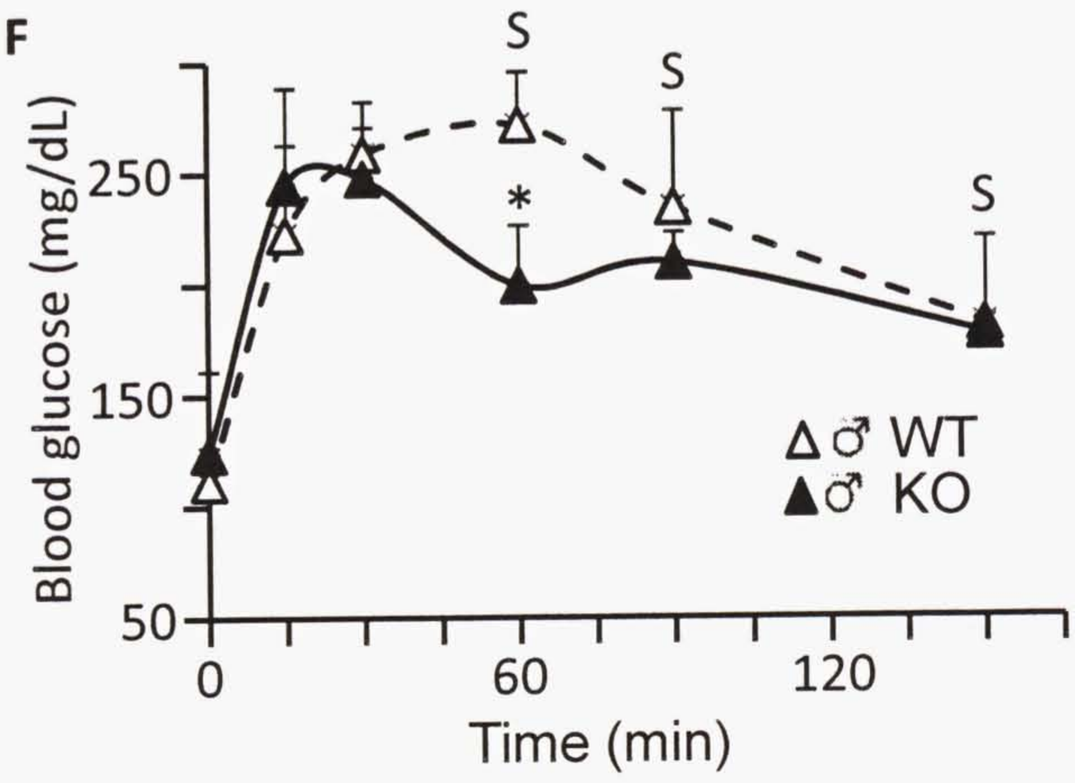

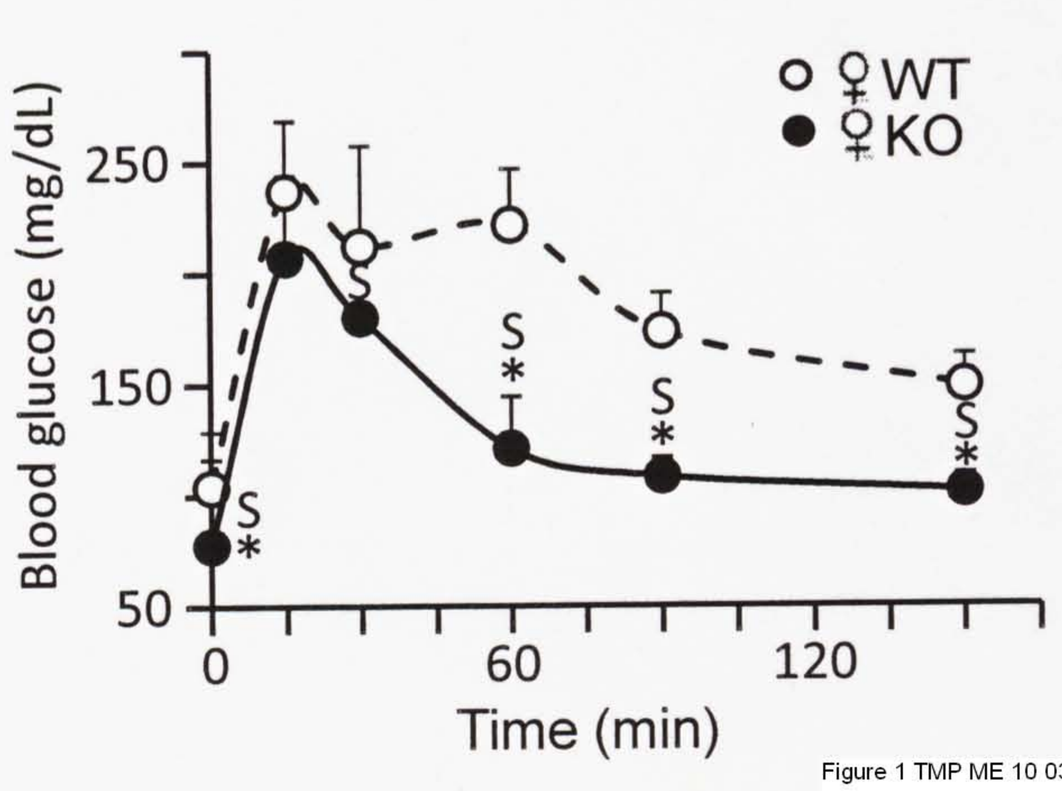

Figure 1 TMP ME 10 0314

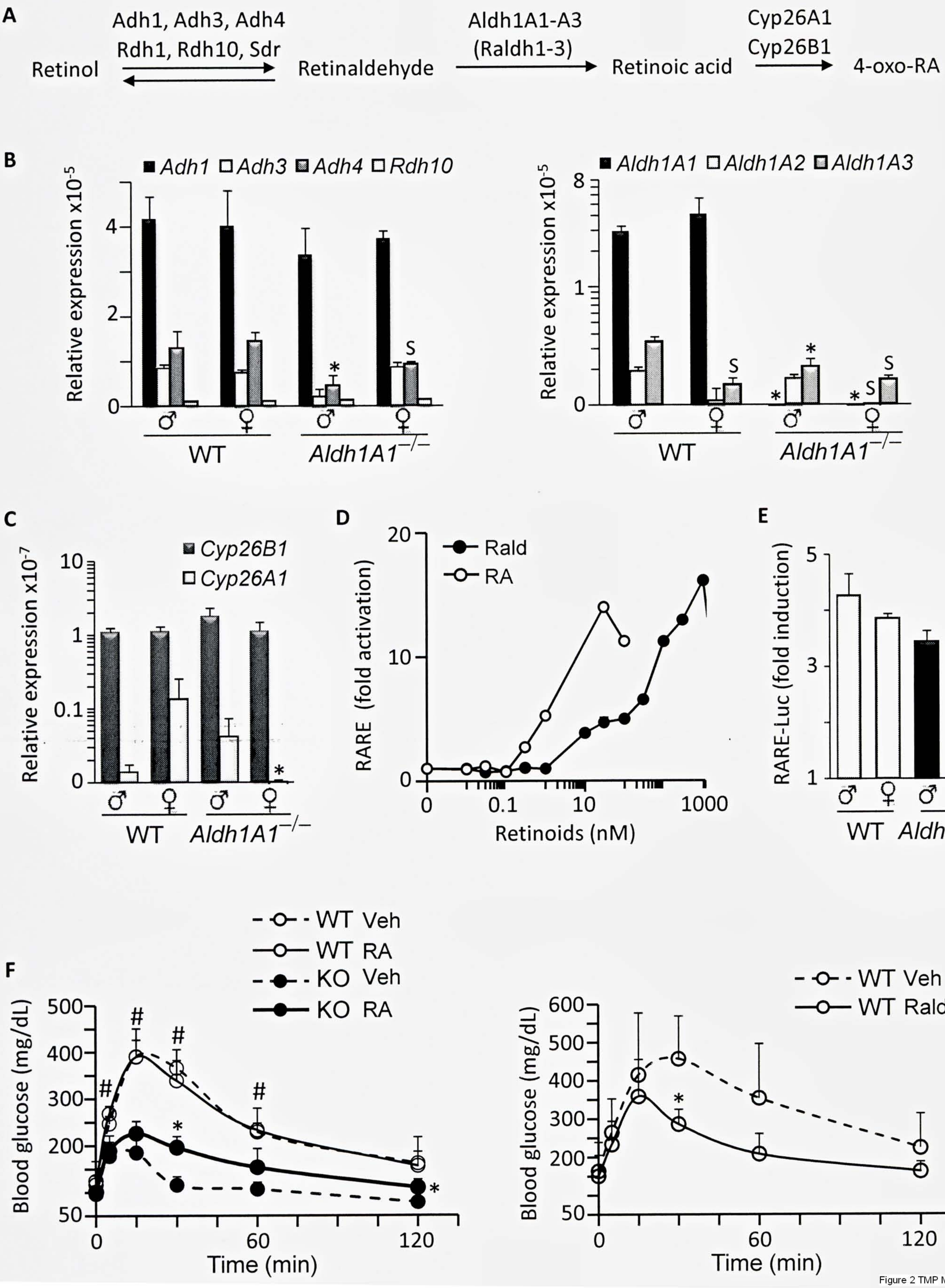

Figure 2 TMP ME 10 0314

A

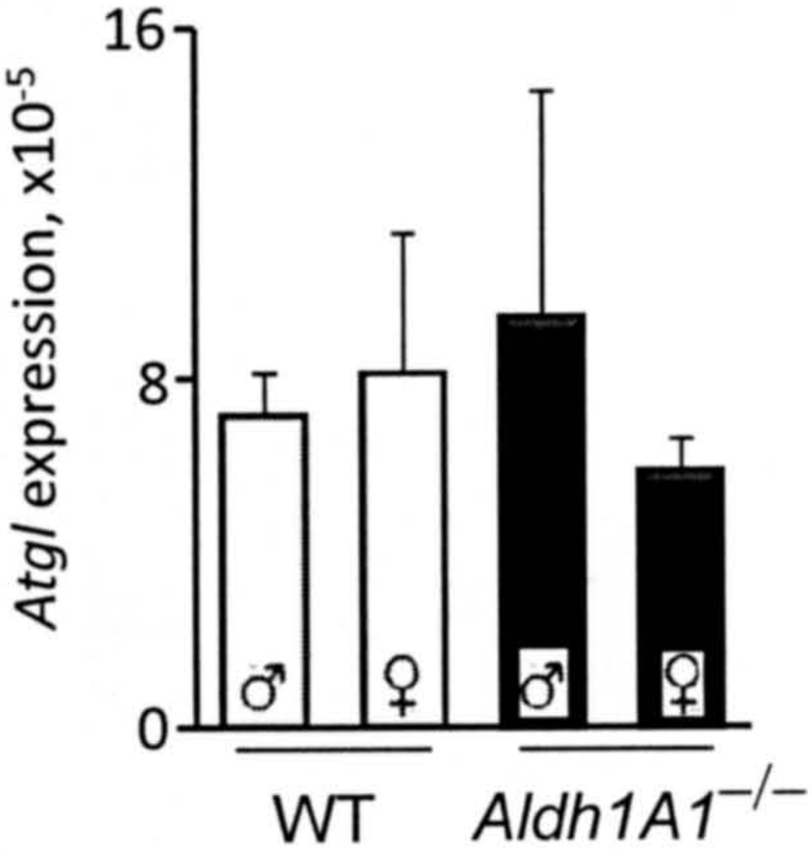

B

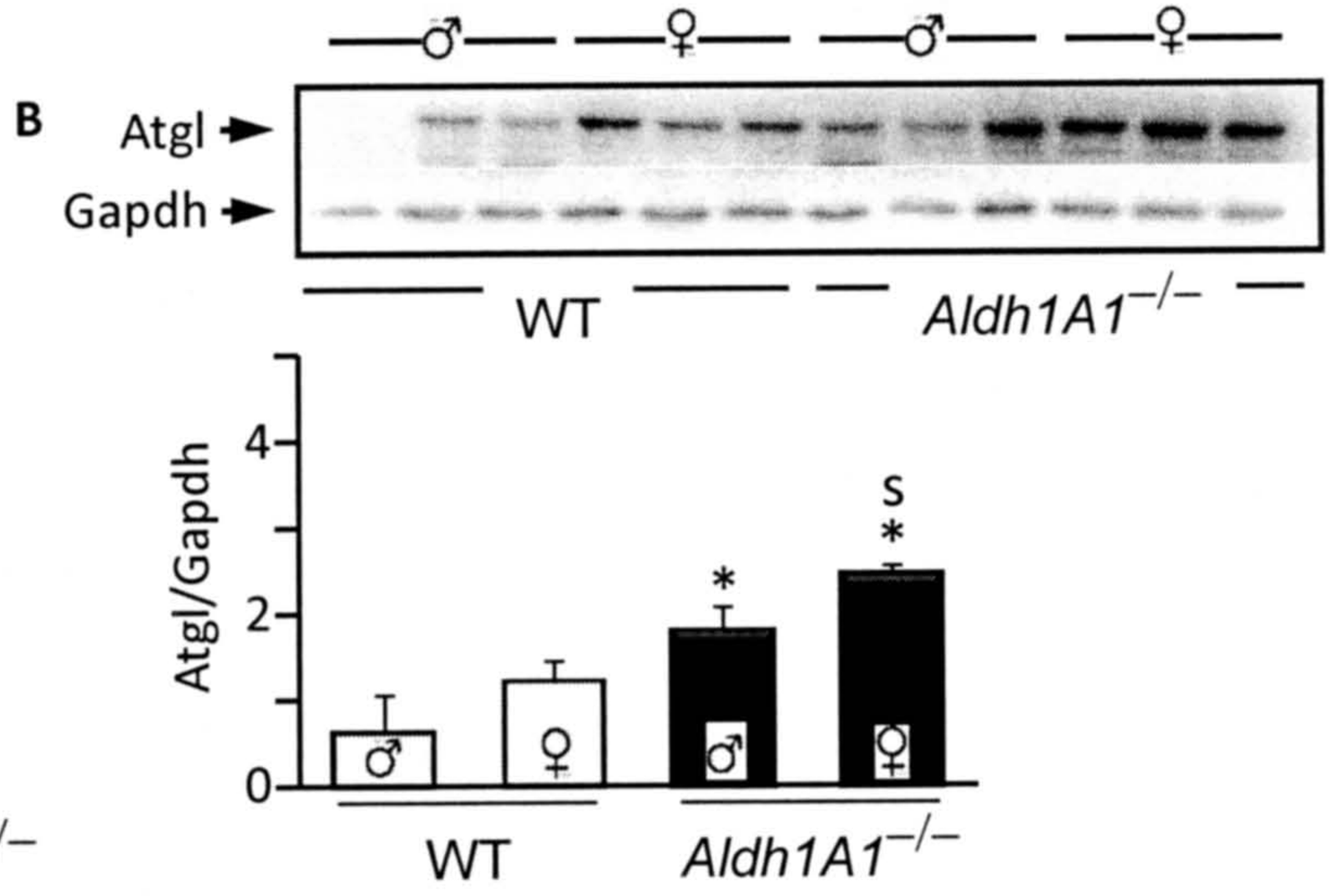

C

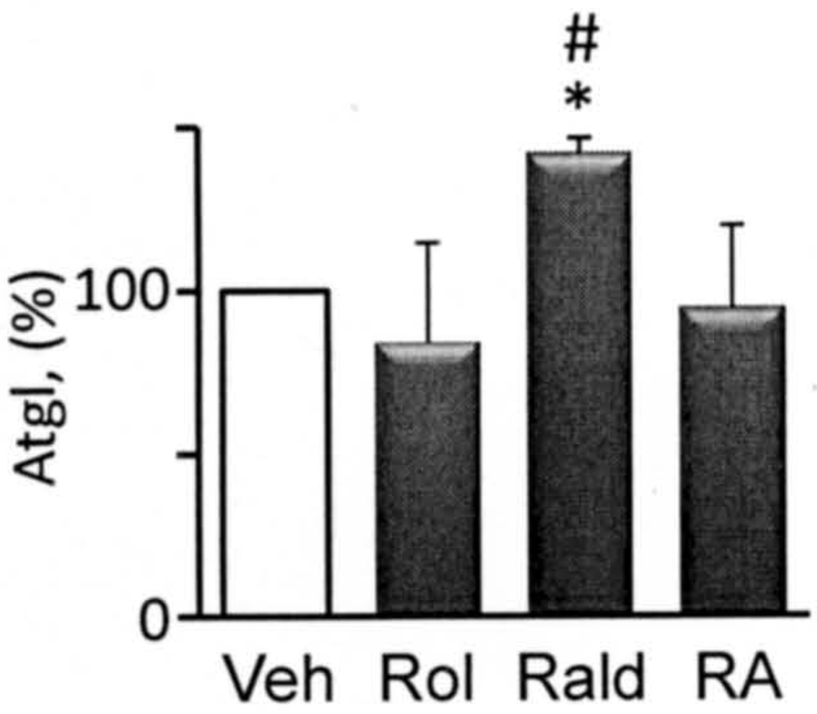

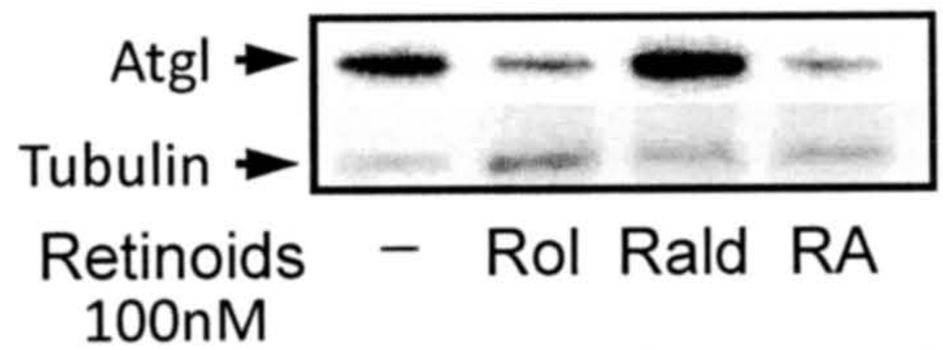

D

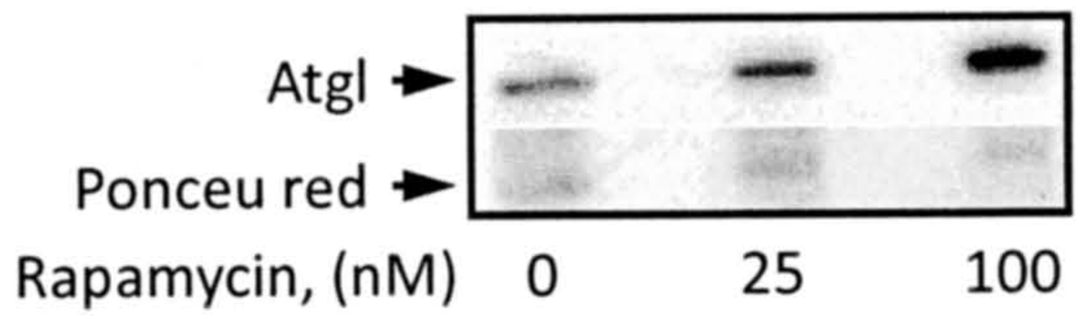

E

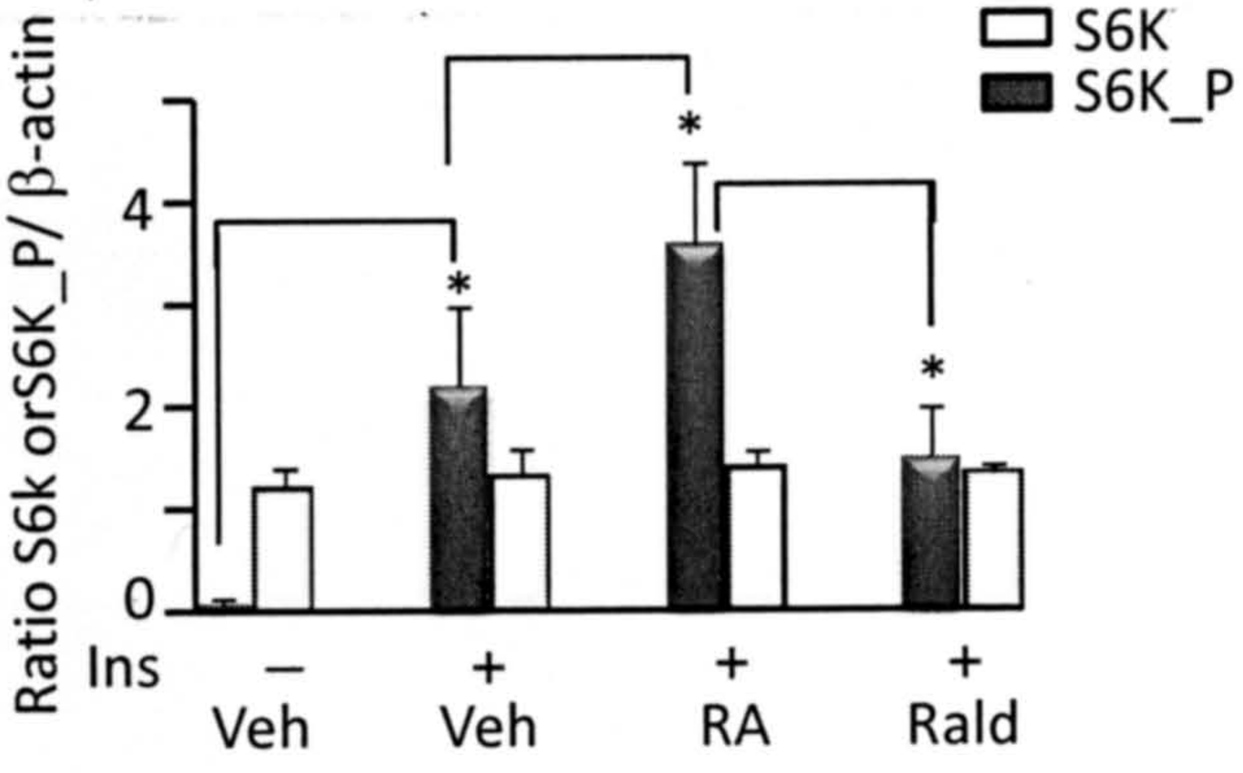

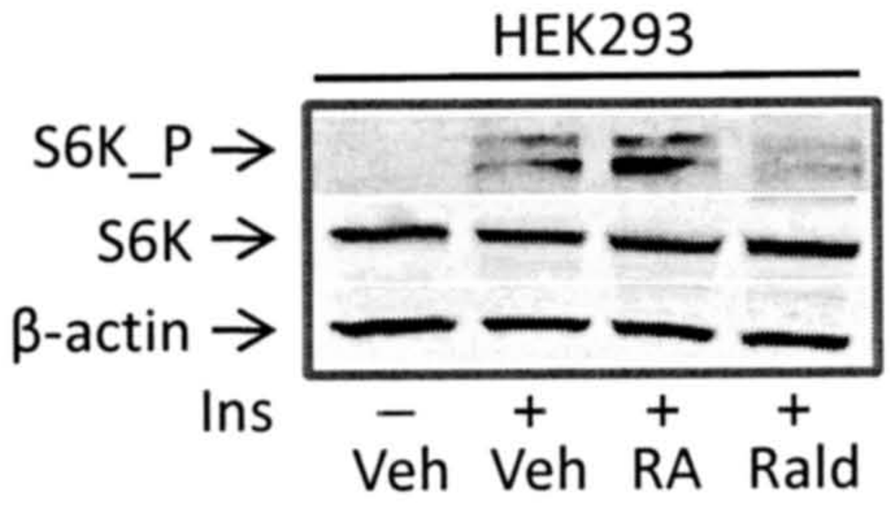

Figure 3 TMP ME 10 0314

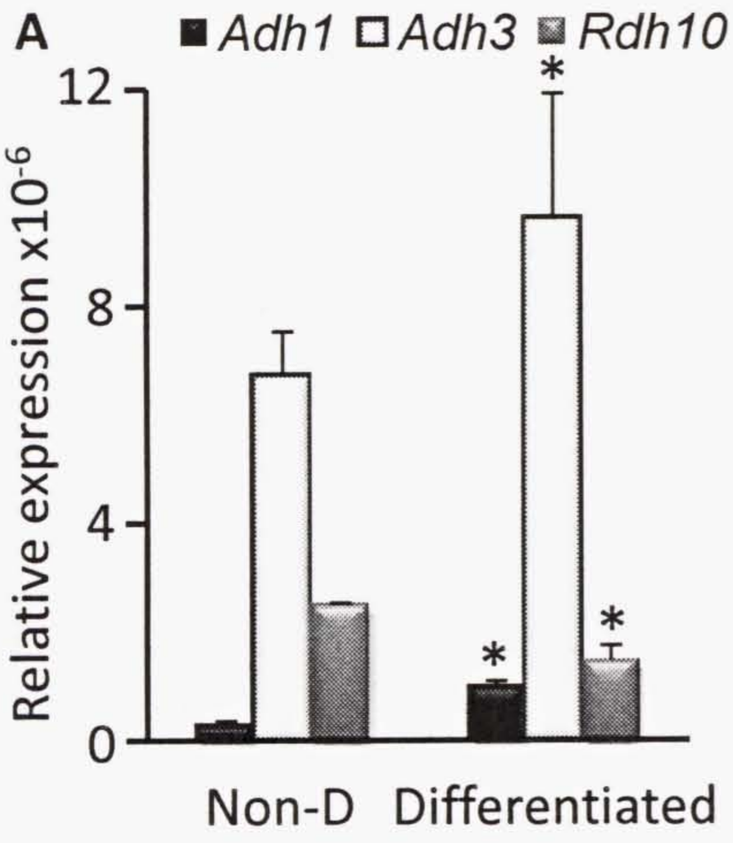

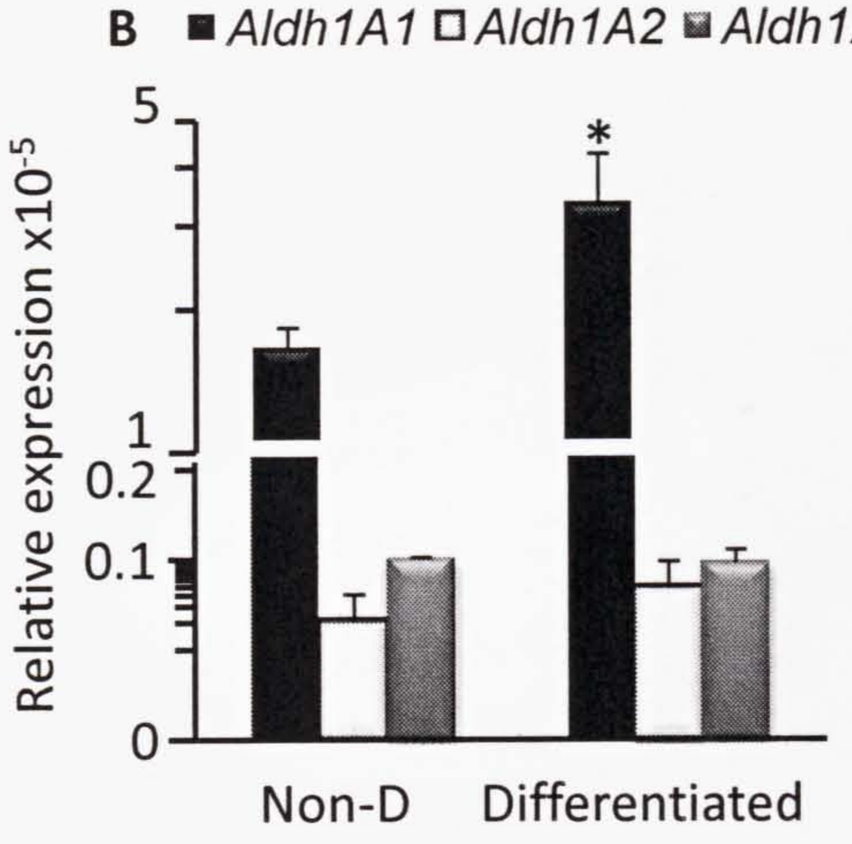

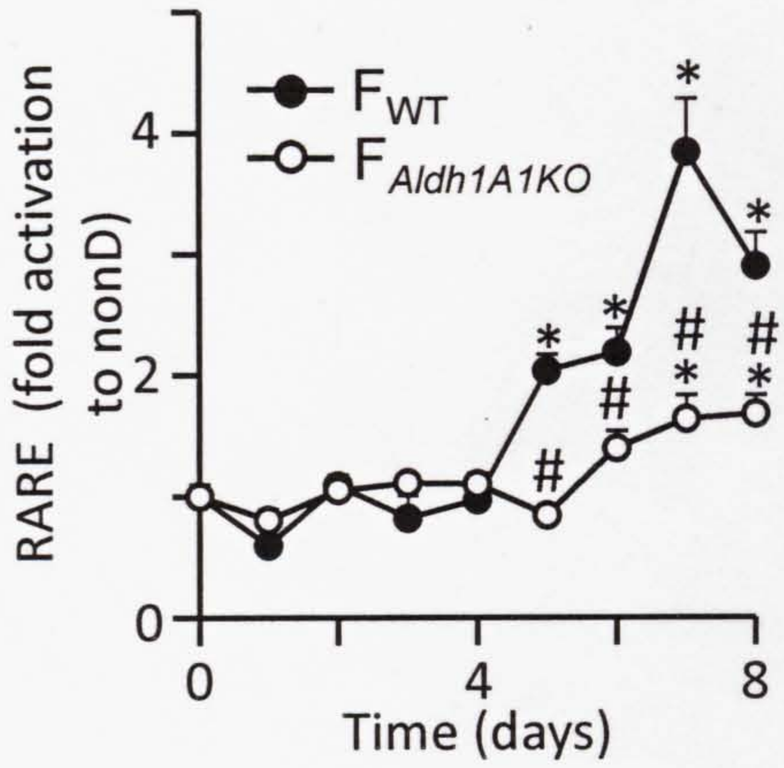

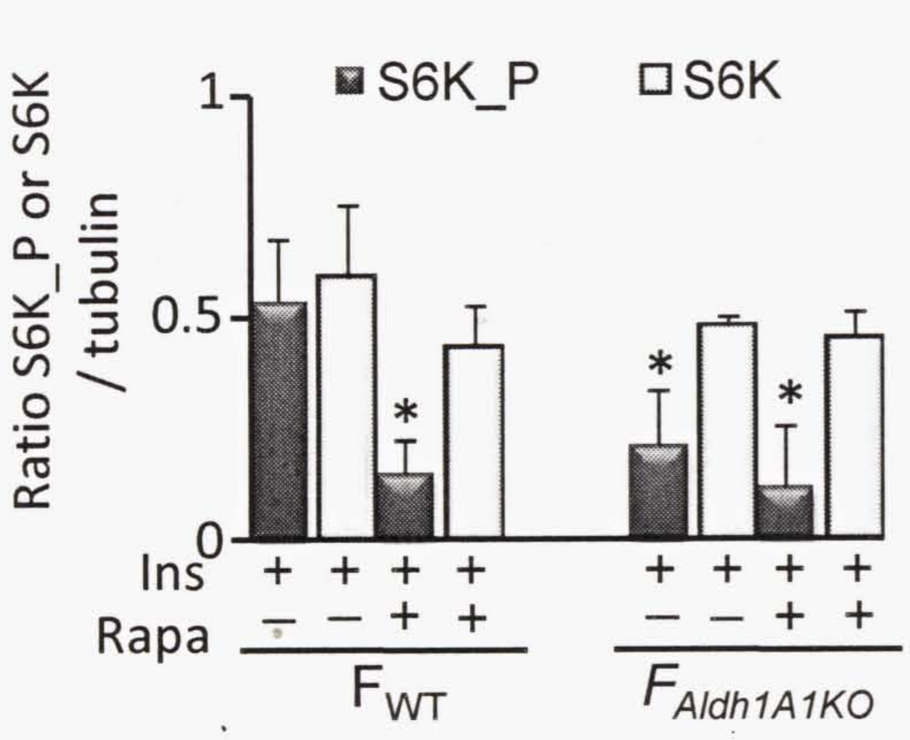

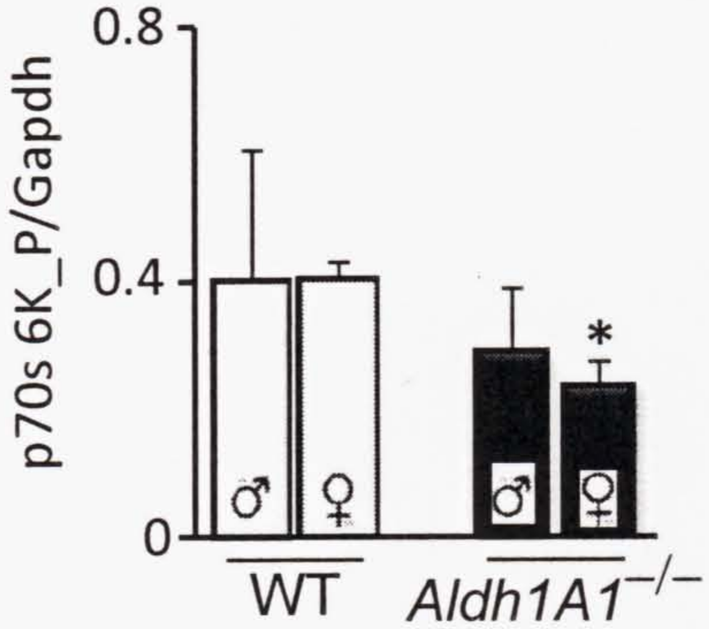

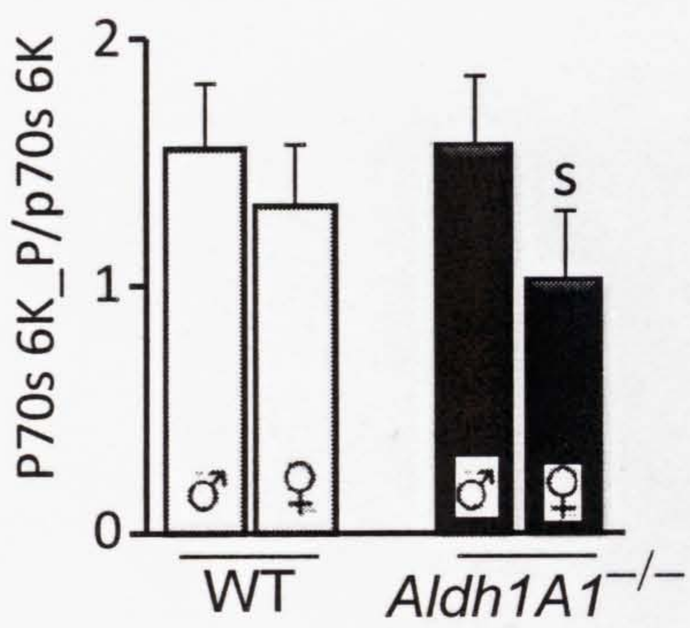

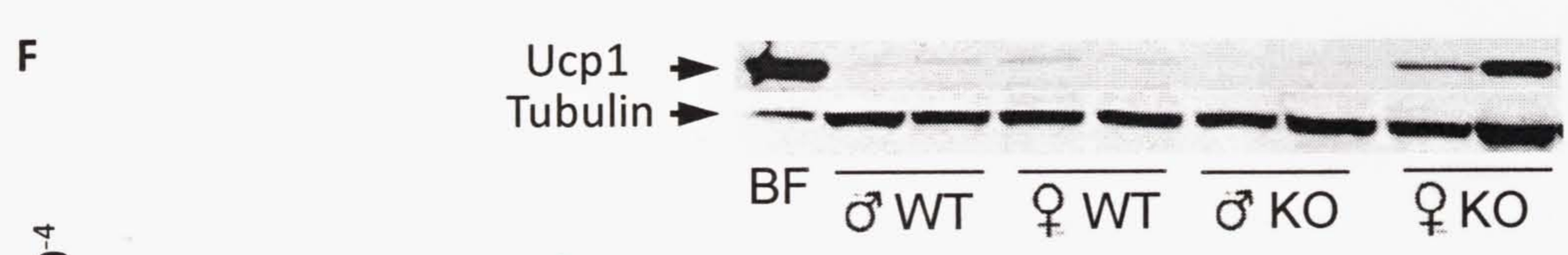

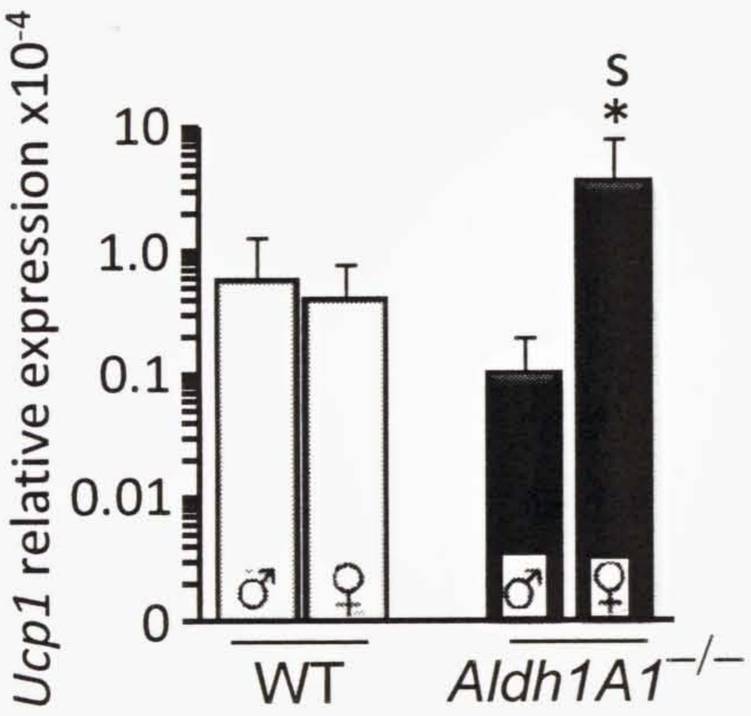

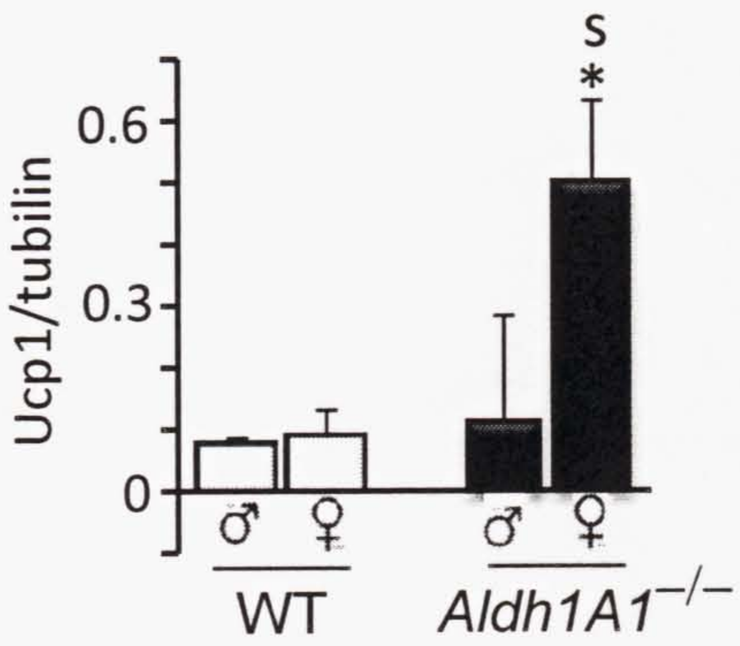

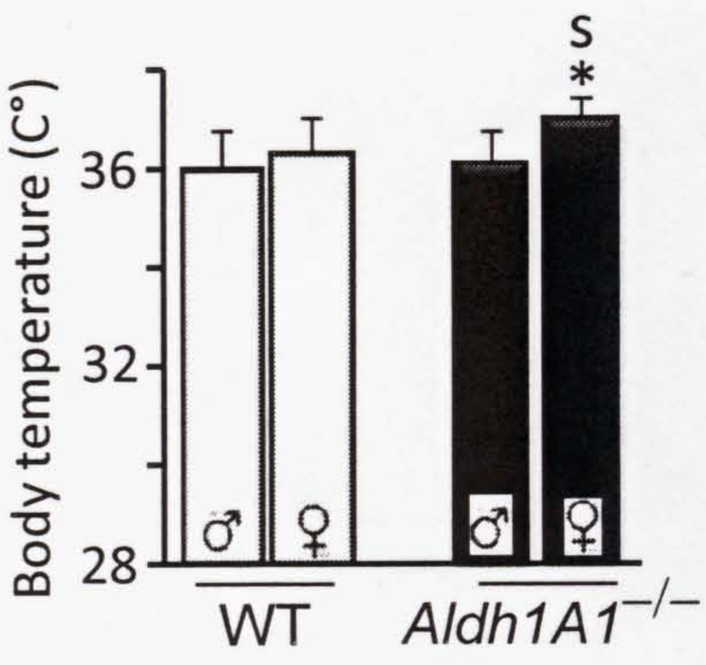

Figure 4 TMP ME 10 0314

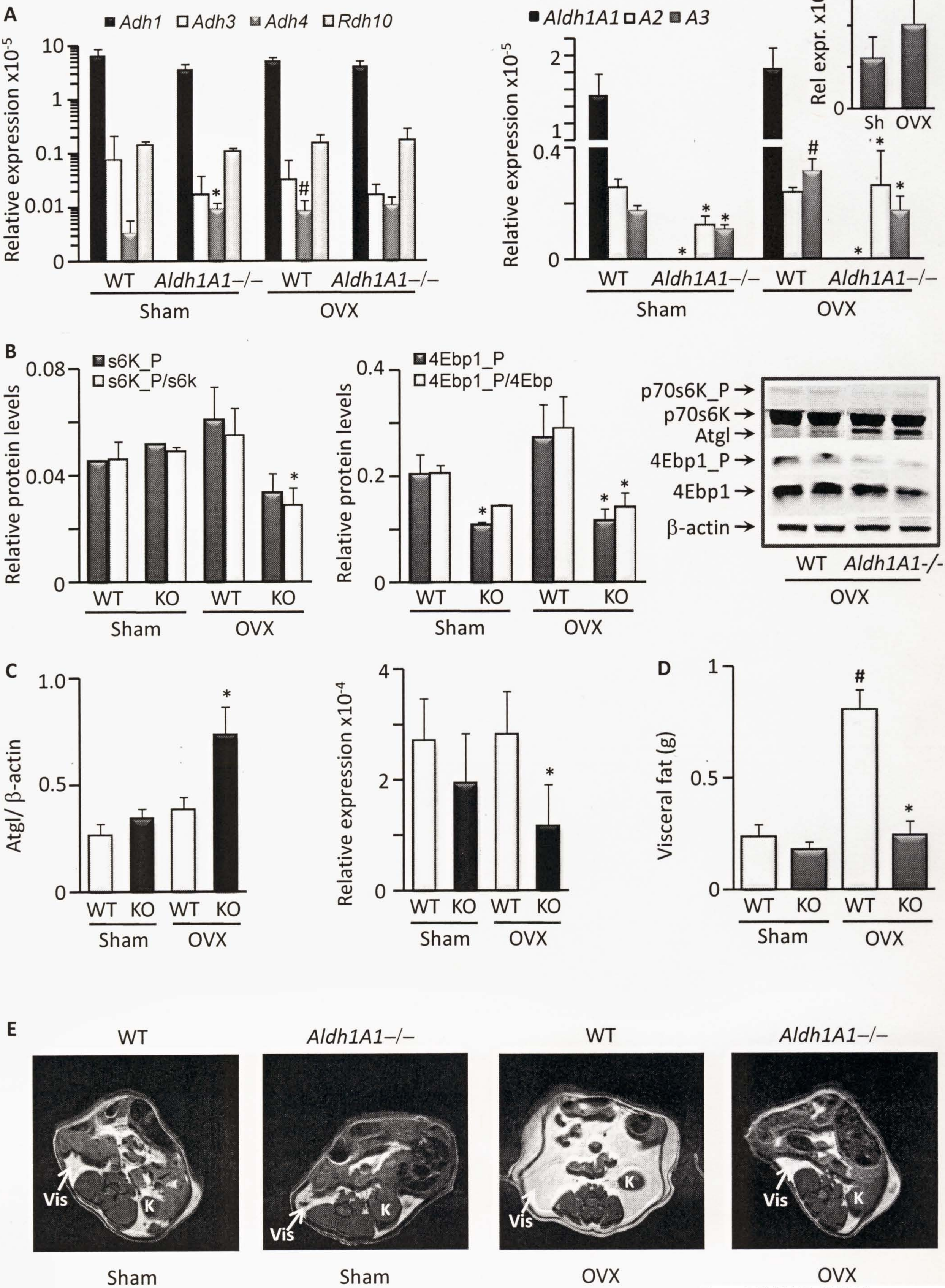

Figure 5 TMP ME 10 0314

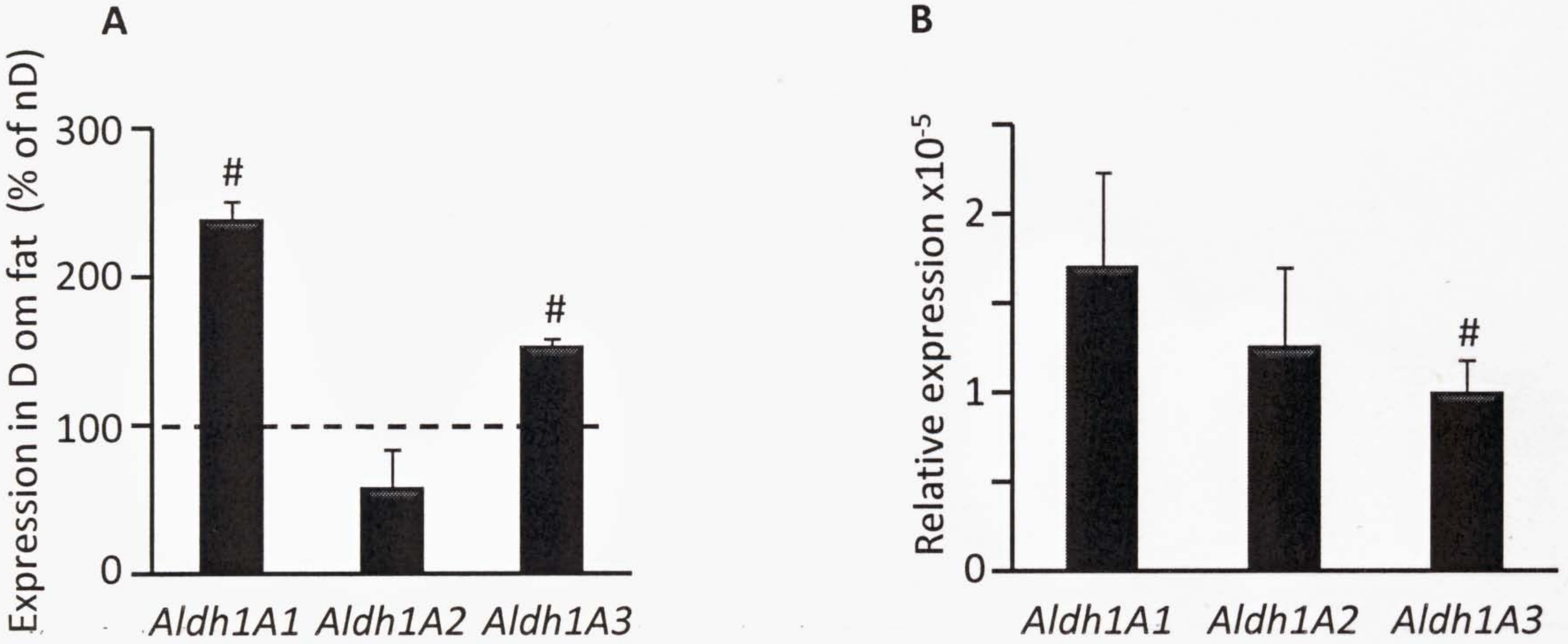

Figure 6 TMP ME 10 0314

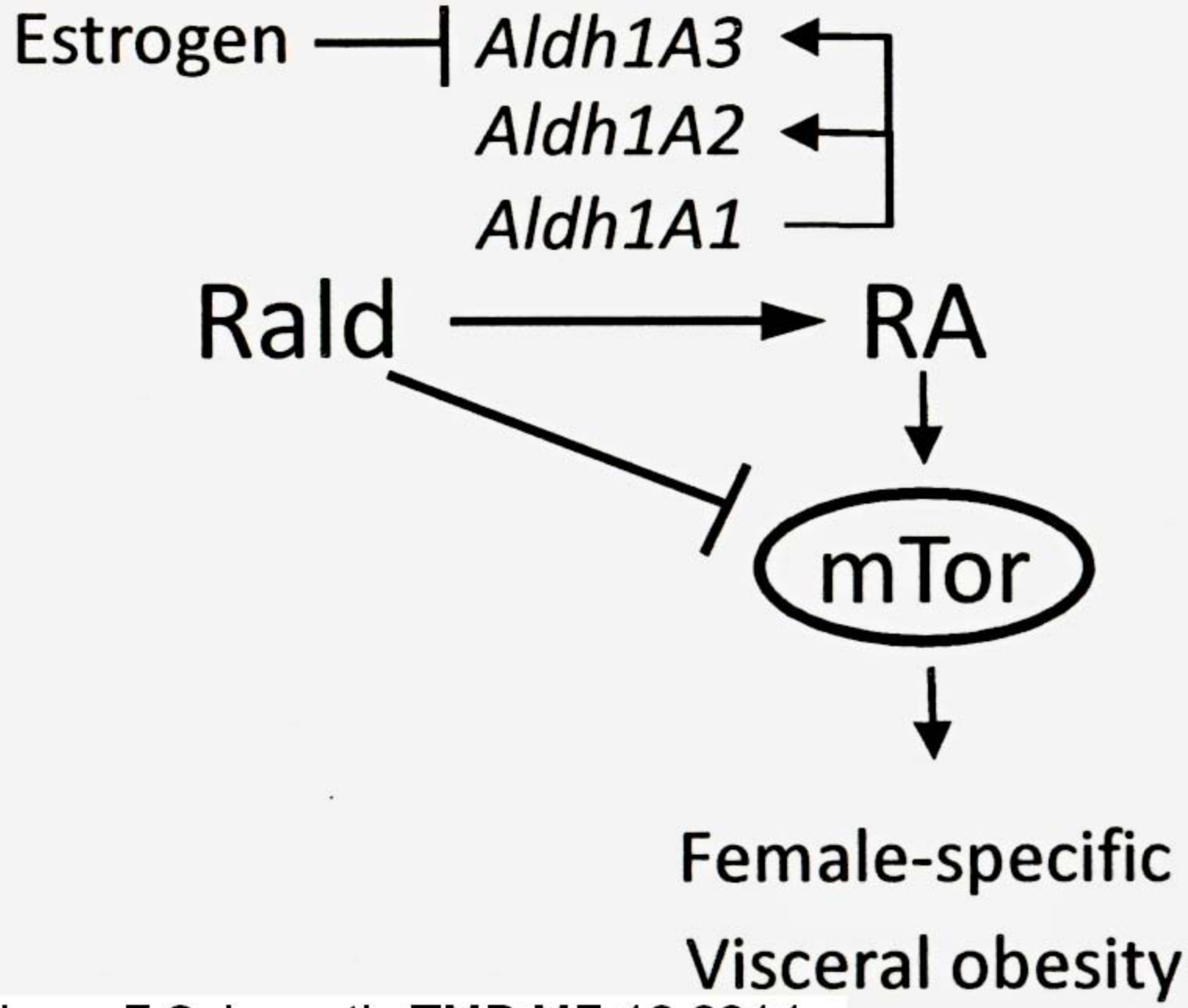

Figure 7 Schematic TMP ME 10 0314

884 **SUPPLEMENTAL INFORMATION**

885 **Figure S1. HF diet did not impair glucose tolerance test in *Aldh1A1*$^{-/-}$ mice; low mRNA expression**
886 **levels of *Rdh1* and *Aldh8A1* in WT and *Aldh1A1*$^{-/-}$ mice on a HF diet**

887 (A) DEXA measurements of fat mass in mice after 180d on HF diet (n=5 in *Aldh1A1*$^{-/-}$ males WT males
888 and females, n=4 in *Aldh1A1*$^{-/-}$ females). Individual values are shown as symbols: triangles,- males (WT
889 white, *Aldh1A1*$^{-/-}$ males black);circles,-females (WT white, *Aldh1A1*$^{-/-}$ males black) *, P<0.05
890 differences between genotypes; S, P<0.05 differences between sexes within one genotype. All data are
891 shown as mean±SD.
892
893 (B) Visceral fat weight in individual *Aldh1A1*$^{-/-}$ males (triangles, n=4 (180 d), n=5 (300d)) and females
894 (circles, n=4 (180d) n=7 (300d)) on a high-fat diet for 180 (white) and 300 days (gray). Lines show
895 mean±SD in each group. *, P<0.05 differences between genotypes; S, differences between sexes within
896 one genotype (*P*<0.008 (180d); *P*<0.028 (130d), both Mann-Whitney U test).
897
898 (C) Relative mRNA expression of Rald reductase *Rdh1* (left panel) and RA-generating *Aldh1A8* (Raldh4)
899 (D). Data are shown as individual values WT male (white triangles, n=5), WT female (n=4, white circles),
900 and *Aldh1A1*$^{-/-}$ male and female mice (black triangles and circles, respectively, both n=4) on a high-fat
901 diet (180days). TaqMan expression data were normalized to 18S expression. Values were not
902 significantly different among groups (Mann-Whitney U test).
903

904 **Figure S2. Validation of RARE assay by RA added in vitro and in vivo**

905 (A) Addition of RA(100nM) to the lipophilic extract (LEA) of visceral adipose tissue activated

RARE-luceferase in a stably transfected fibroblast clone. All procedures were performed under argon atmosphere in the dark. Visceral adipose tissue was dissected from a WT male (on HF diet 180 days) and homogenized in RIPA buffer. Lipophilic extracts (5µg protein/50mL ethanol) were prepared from 100µL of adipose tissue homogenate in the absence (LEA) and in the presence of RA(100nM) (LEA+RA), as well as with RA (RA, 100nM) extracted using similar procedure. Data were normalized to RARE luciferase activity seen in the non-treated cells. Data are shown as mean±SD of three independent experiments. *, P<0.05 compared to control, Mann-Whitney U test.

(B) Retinol concentration in lipophilic extracts from plasma from WT male (n=5), WT female (n=4), and *Aldh1A1*$^{-/-}$ male and female mice (both n=4) measured using HPLC method as described in (23) and Supplementary materials. Values were not significantly different among groups (Mann-Whitney U test).

(C) RARE activation by serum (% in culture medium) isolated from WT male mouse 10 minutes after intraperitoneal injection with 1mL PBS (white bar, 0.5% serum) and 1mL PBS containing 500nM RA (black bars, 0.5 and 1% serum). For comparison cells also were treated with RAR ligand TTNPB (1nM). Data were normalized to RARE luciferase activity seen in the non-treated cells. Data are shown as mean±SD of three independent experiments. *, *P*<0.05 compared to control, Mann-Whitney U test.

Figure S3. Representative DIGE gel image overlays for male WT and *Aldh1A1*$^{-/-}$ (labeled with cy3 and cy5 dyes) proteins (left panel) as well as for female WT and *Aldh1A1*$^{-/-}$ (labeled with cy3 and cy5 dyes) proteins (right panel)

Proteins were homogenate of visceral adipose tissue from a study described in Figure 1 (180d). Each DIGE gel was performed 4 times with different WT and *Aldh1A1*$^{-/-}$ male or female pair of mice. Arrow shows and example of a protein varied in male WT and *Aldh1A1*$^{-/-}$ pair, but is absent in a female pair. Statistical analysis (independent *T*- test) was performed to identify spots that were significantly (*P*<0.05, n=4) different between groups (WT and *Aldh1A1*$^{-/-}$). Significant spots were further filtered to identify

spots with more than 1.5 fold differences in abundance, and spots appeared in at least 3 of the 4 gels. 176 spots were different between WT and *Aldh1A1*$^{-/-}$ mice without FDRC in male and 167 spots in female groups. Only proteins that were significantly different between WT and *Aldh1A1*$^{-/-}$ mice after FDRC analysis were spotted and identified. We defined them as **proteomic markers** in this paper. Of note, that many proteomic markers were changed in both male and female groups (Table 1, Group 1). Some of proteomic markers were only significantly changed in males (Table 1, Group 2) or in females (Table 1, Group 3).

Figure S4. mRNA expression levels of nuclear receptors (*Pparγ, RXR*), Pparγ target gene (*Fabp4*), genes activated by Pparγ ligands (*vaspin, caspase-1*) and or RA (*leptin, caspase-1*) in visceral fat of WT and *Aldh1a1*$^{-/-}$ mice.

Data are shown as individual values WT male (white triangles, n=5), WT female (n=4, white circles), and *Aldh1A1*$^{-/-}$ (KO) male and female mice (black triangles and circles, respectively, both n=4) on a high-fat diet (180days). TaqMan expression data were normalized to 18S expression. *, values were significantly different between WT and KO male or female groups (Mann-Whitney U test). Changes between WT males and females as well between KO males and females were not statistically significant (Mann-Whitney U test).

Figure S5. Impaired differentiation in *Aldh1A1*$^{-/-}$ *vs*. WT adipocytes and the opposite effects of RA *versus* Rald and rapamycin effects on mTOR activation in cultured adipocytes

(A) Differentiated (7d) *Aldh1A1*$^{-/-}$ *vs*. WT adipocytes were analyzed for mRNA expression of *Fabp4* and *Pref1* that are markers of differentiated and non-differentiated adipocytes, respectively. Data are shown as ratio of *Pref1* to *Fabp4* expression. Values are mean±SD of three independent experiments. *, $P<0.05$, Mann-Whitney U test.

(B-D) Representative western blots of S6K_P and p70S6 kinase levels in differentiated (5d) 3T3-L1 (B, C) and WT (D) fibroblasts stimulated with 100nM insulin/20%FBS (ins, 30min) with or without rapamycin (rapa), RA, and Rald (all 100nM, added 10min after ins). Prior to stimulation cells were starved.

Figure S6. *Aldh1A1*$^{-/-}$ female mice resist weight gain induced by ovariectomy

(A) Body weight and (B) food intake in sham-operated (n=5) and ovariectomized (OVX, n=4, mean±SE) WT and *Aldh1A1*$^{-/-}$ female mice on regular chow. # $P<0.05$ differences between sham and ovariectomized, * differences between ovariectomized WT and *Aldh1A1*$^{-/-}$ mice.

METHODS

Human subjects

mRNA was isolated from visceral (omental) fat tissue, which was obtained from healthy women who underwent surgery as kidney donors and had given informed consent. The protocol was approved by the Mayo Clinic Institutional Review Board for Human Research. All subjects had fasted at least 12 h. Subjects were 41 ± 2 yr of age. The subjects' mean body mass index (BMI) was 30.3± 0.4 kg/m^2. Patients' fasting plasma glucose concentrations did not exceed 120 mg/dL, they were not taking thiozolidinediones (glitazones) or steroids, and they had no reported malignancies. Abdominal subcutaneous (external to the fascia superficialis) and greater omental fat were obtained from each subject.

Preadipocyte culture

Fat tissue was minced and then digested in phosphate buffered saline (PBS) containing 1 mg/ml collagenase in a shaking water bath (37°C). Digests were filtered and centrifuged at 800 g for 10 min. The

digests were treated with an erythrocyte lysis buffer and then plated in alpha minimal essential medium (α-MEM) supplemented with 10% bovine serum and antibiotics. To eliminate endothelial cell and macrophage contamination, the adherent preadipocytes were replated after 12 h at a density of 4 ± 104 cells/cm2 in plating medium as described before (50). The absence of macrophages in subcultured preadipocytes was confirmed by absence of macrophage markers assayed by quantitative RT-PCR. Preadipocytes were differentiated as described previously (50) using plating medium without serum supplemented with 100 nM dexamethasone, 500 nM human insulin, 200 pM triiodothyronine, 0.5 μM rosiglitazone, antibiotics, and 540 μM isobutylmethylxanthine (removed after 2 days). Cells were differentiated for 21days. Medium was changed weekly.

Magnetic resonance imaging (MRI)

MRI of intraperitoneal area was performed as described (48), using a Bruker 11.7T NMR system (Bruker Instruments) with a 11.7-T Bruker magnet and a 52mm internal diameter vertical bore (Bruker Instruments, Billerica, MA) (500 MHz/gradient strength of 300 gauss/cm). We measured fat accumulation with a T1-weighted gradient-echo sequence on mice at the end of the study. We obtained and analyzed twenty-five contiguous, 1-mm thick axial GRE slices spanning from the superior pole of the uppermost kidney to the caudal aspect of the mouse using a spin-echo sequence with a 256 X 256 matrix size (pixel size, 117 x117 x 1,000 μm^3).

Proteomic analysis

Sample preparation

Samples were resuspended in DIGE labeling buffer (30mM TRIS, 7M urea, 2M thiourea, 2% CHAPS, pH 8.5) and protein concentrations were measured by Bradford assay. For each of the experiments, 94μg per sample was used for DIGE labeling, with 62.66μg cy3 or cy5 labeled, and 31.34μg from each sample combined as an internal standard and labeled with cy2. Samples, labeled DIGEfluor minimal-label dyes,

were combined for appropriate gels and diluted with rehydration buffer (7M Urea, 2M thiourea, 4% CHAPS, 10mg/ml DTT, 1% pH 4-7 IPG buffer, 0.1% bromophenol blue). Samples were immediately used to rehydrate 18cm pH 4-7 Immobiline dry strip isoelectric focusing strips under mineral oil overnight. Subsequently, the strips were focused using an IPGphor II IEF. Focus strips were equilibrated in EQ buffer 1 (50mM tris pH 8.8, 6M urea, 30% glycerol, 0.1% bromophenol blue, 2% SDS, 65mM DTT) for 15 minutes, followed by EQ buffer 2 (50mM tris pH 8.8, 6M urea, 30% glycerol, 0.1% bromophenol blue, 2% SDS, 135mM iodoacetamide) for 15 minutes. Strips were immediately placed in 12% 20X24cm lab-cast gels, sealed in place using agarose, and run on a Dalt12 electrophoresis system following standard protocols. Proteomic analysis as performed at CCIC Mass Spec and Proteomics facility, the Ohio State University Medical Center.

After SDS-PAGE, gels were immediately scanned 3 times in a Typhoon using appropriate settings for each DIGE fluorophor. DIGE images were loaded into Decyder 2D 6.5 for analysis. Individual gels (containing 1 each of cy2, cy3, and cy5 images) were spot mapped using the Decyder Differential Image Analysis Module. Dust and saturated spots were filtered out manually. All images from the experiment (4 sets each) were then loaded into the Decyder Biological Variation Analysis software and internal standard (cy2) images were matched. Matching images were grouped accordingly. Statistical analysis (independent *T* test) was performed to identify spots that were significantly ($P<0.05$) different between groups (WT and *Aldh1A1*$^{-/-}$). Significant spots were further filtered to identify spots with more than 1.5 fold differences in abundance, and spots appeared in at least 3 of the 4 gels. False discovery rate correction was applied to identify further the most likely biologically significant differences. We identified 176 spots in male and 167 spots in female groups that were different between WT and *Aldh1A1*$^{-/-}$ mice without FDRC. Only proteins that were significantly different between WT and *Aldh1A1*$^{-/-}$ mice after FDRC analysis were spotted and identified. We defined them as **proteomic markers** in this paper.

Significantly changed spots were matched between analytical gels and preparative gels, and then cored from preparative gels using an Ettan Spot Handling Workstation 2.1. Spots were washed with water, dried with acetonitrile, and digested with Trypsin overnight in a 96 well plate. Peptides were extracted with 50% acetonitrile/5% formic acid and concentrated.

Mass Spectrometer LTQ

Samples were identified using capillary liquid-chromatography-nanospray tandem mass spectrometry (Nano-LC/MS/MS), which was performed on a Thermo Finnigan LTQ mass spectrometer equipped with a nanospray source operated in positive ion mode. The LC system was an UltiMate™ 3000 system from Dionex (Sunnyvale, CA). Solvent A was water containing 50mM acetic acid and Solvent B was acetonitrile. 5 microliters of each sample was first injected onto the µ-Precolumn Cartridge (Dionex, Sunnyvale, CA) and washed with 50 mM acetic acid. The injector port was switched to inject and the peptides were eluted off of the trap onto the column. A 5 cm 75 µm ID ProteoPep II C18 column (New Objective, Inc. Woburn, MA) packed directly in the nanospray tip was used for chromatographic separations. Peptides were eluted directly off the column into the LTQ system using a gradient of 2-80%B over 45 minutes, with a flow rate of 300 nl/min. The total run time was 65 minutes. The MS/MS was acquired according to standard conditions established in the lab. Briefly, a nanospray source operated with a spray voltage of 3 KV and a capillary temperature of 200PoPC is used. The scan sequence of the mass spectrometer was based on the TopTen™ method; the analysis was programmed for a full scan recorded between 350 – 2000 Da, and a MS/MS scan to generate product ion spectra to determine amino acid sequence in consecutive instrument scans of the ten most abundant peaks in the spectrum. The CID fragmentation energy was set to 35%. Dynamic exclusion is enabled with a repeat count of 30 s, exclusion duration of 350 s, and a low mass width of 0.5 Da and high mass width of 1.50 Da.

Sequence information from the MS/MS data was processed by converting the raw data files into a merged file (.mgf) using an inhouse program, RAW2MZXML_n_MGF_batch (merge.pl, a Perl script). The

resulting mgf files were searched using Mascot Daemon by Matrix Science version 2.2.1 (Boston, MA) and the database searched against the full SwissProt database version 54.1 (283454 sequences; 104030551 residues). The mass accuracy of the precursor ions was set to 2.0 Da given that the data were acquired on an ion trap mass analyzer and the fragment mass accuracy was set to 0.5 Da. Considered modifications (variable) were methionine oxidation and carbamidomethyl cysteine. Two missed cleavages for the enzyme were permitted. Peptides with a score less than 20 were filtered and proteins identified required bold red peptides. Protein identifications were checked manually and proteins with a Mascot score of 50 or higher with a minimum of two unique peptides from one protein having a -b or -y ion sequence tag of five residues or better were accepted. Peptide mass fingerprinting and quadruple time-of-flight tandem mass spectrometry showed that five proteins were present in two different modifications. Although important, the modification phenomena are beyond the scope of this study and will not be examined and verified here. Expression of proteomic markers was further verified using western blot or TaqMan analysis of mRNA expression using visceral fat from the same mice.

High-performance liquid chromatography (HPLC)

All procedure were performed under argon or nitrogen; samples were protected from light. Blood was collected in the presence of 0.25μM EDTA by cardiac puncture. Plasma (200μL) was reduced in hydroxylamine (1M in100 μL methanol) in PBS (400 μL) for 1h at room temperature. Then ethanol (400 μL) and hexane (4mL) was added and lipid fraction was extracted. We evaporated the hexane phase under nitrogen, then resuspended in ethanol. Retinol was eluted fromPecosphere-3 C18 0.46x8.3cm cartridge column (Perkin-Elmer, Inc., Norwalk, CT) using a mobile phase containing acetonitrile /tetrahydrofuran/water (solvent A, 50:20:30 v/v/v, solvent B 50:44:6 v/v/v) at 1mL/min flow. Retinol was detected with a photodiode array detector (Waters 996)43. We analyzed samples using an external standard (500nM all-*trans* retinol, Sigma-Aldrich).

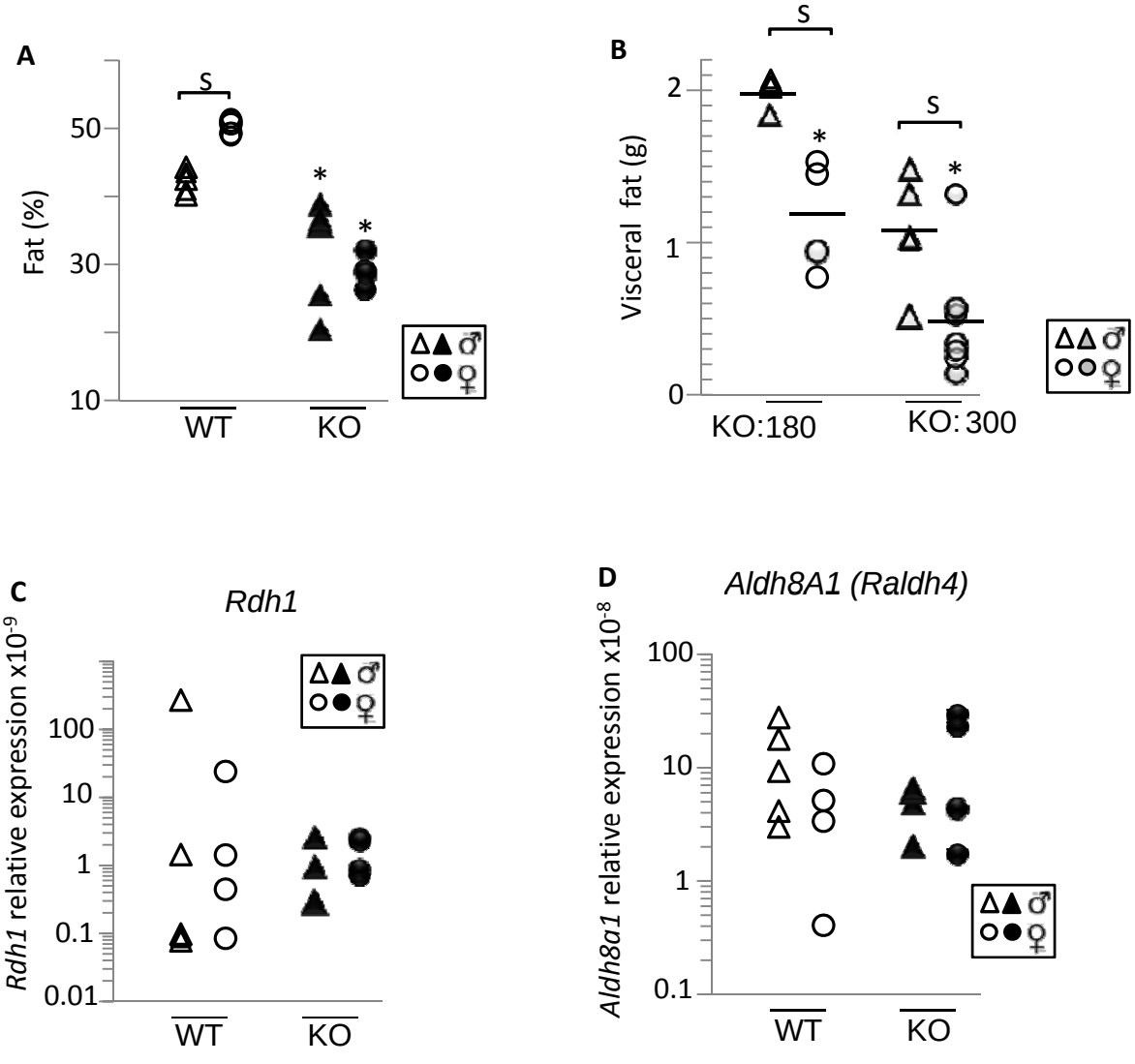

TMP ME 10 0314 FIGURE _S1

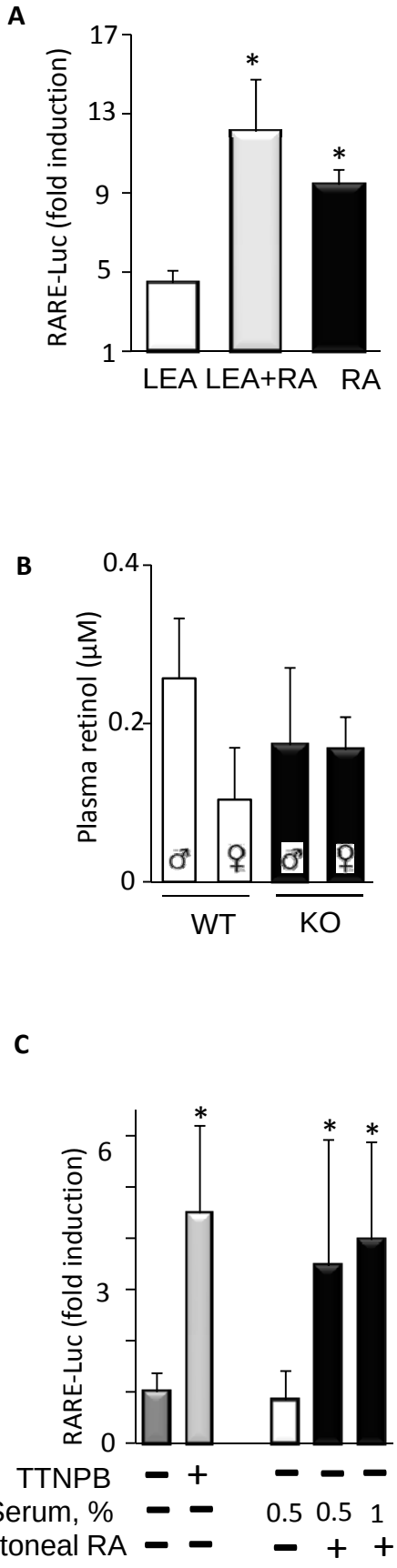

TMP ME 10 0314 FIGURE _S2

WT and KO ♂

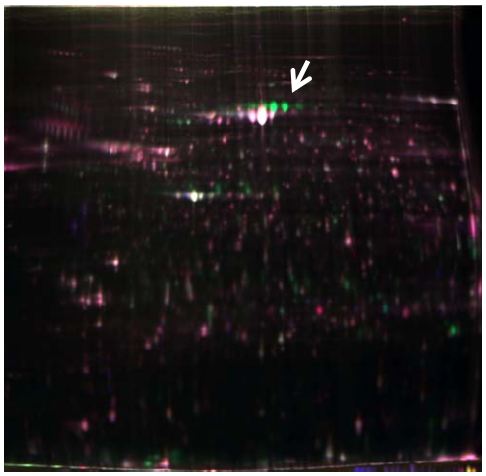

WT and KO ♀

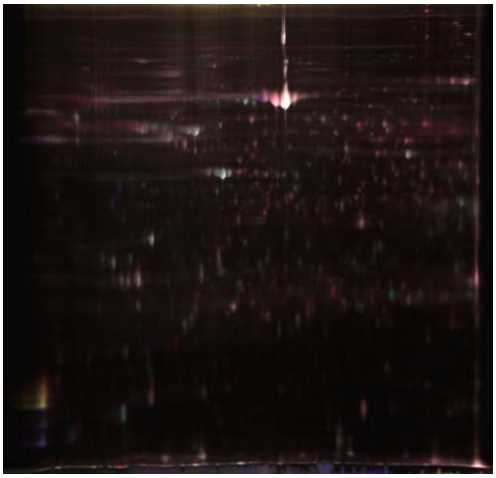

TMP ME 10 0314 FIGURE _S3

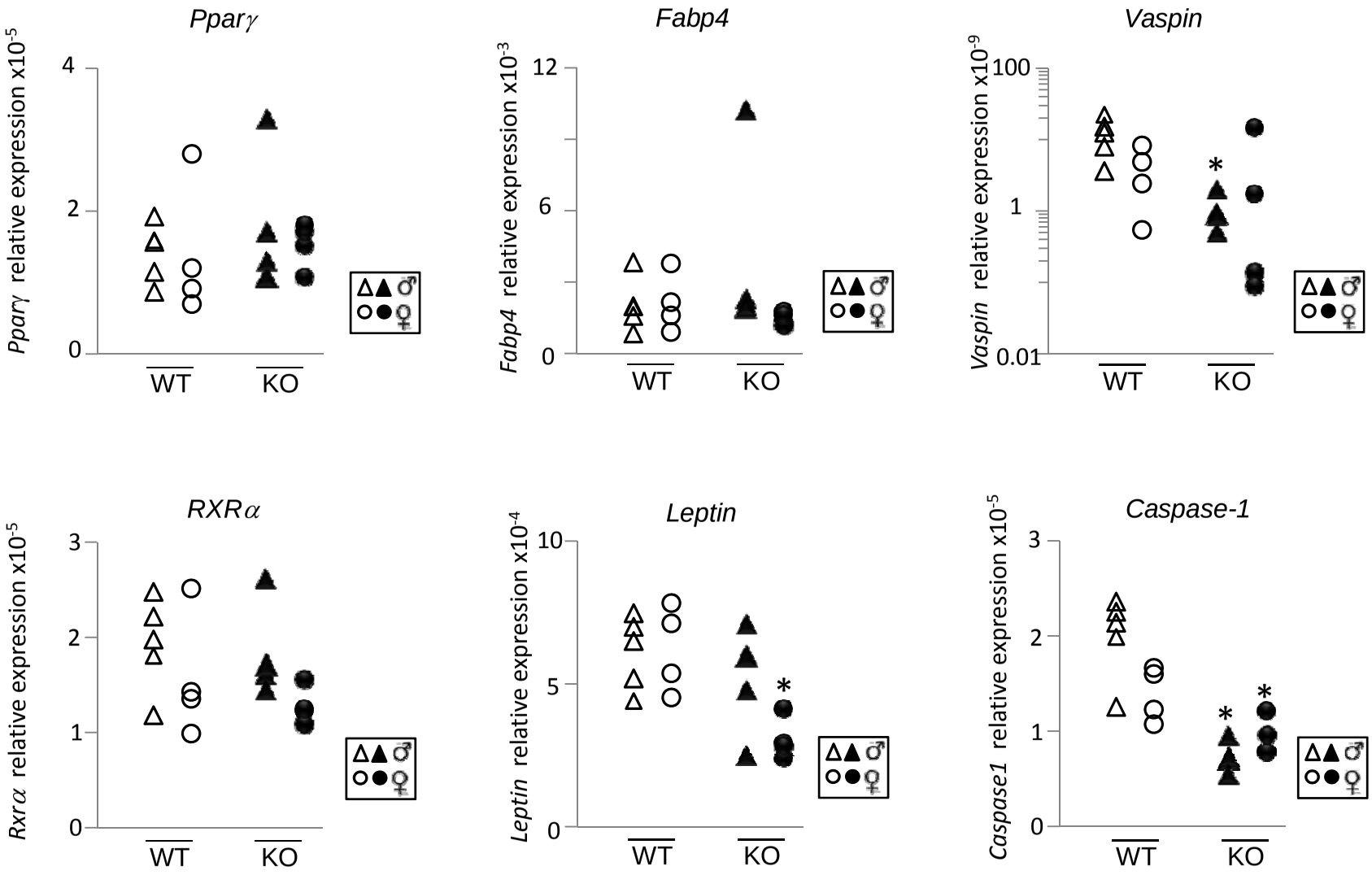

TMP ME 10 0314 FIGURE _S4

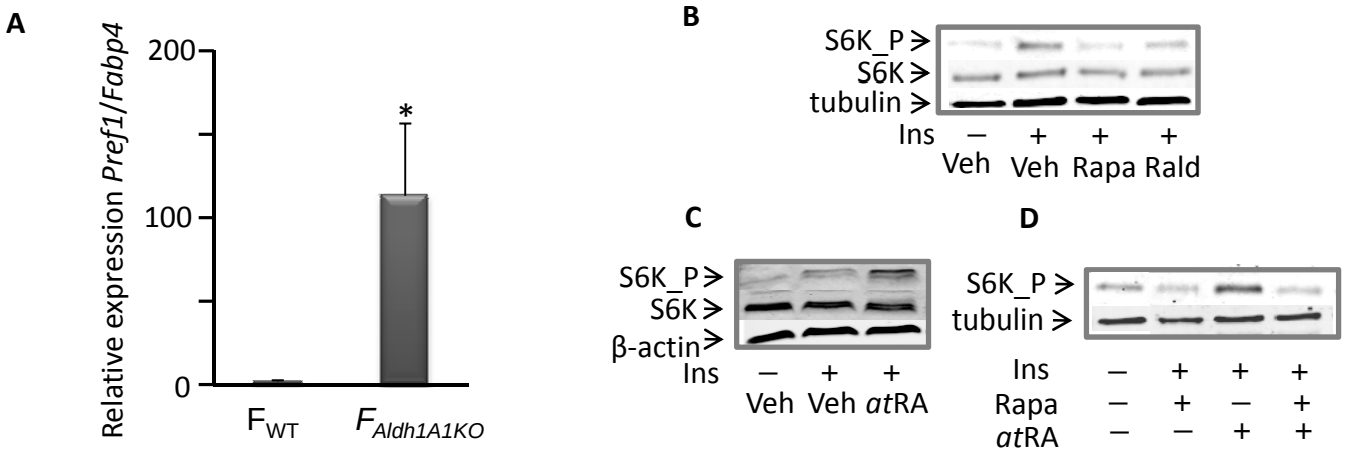

TMP ME 10 0314 FIGURE _S5

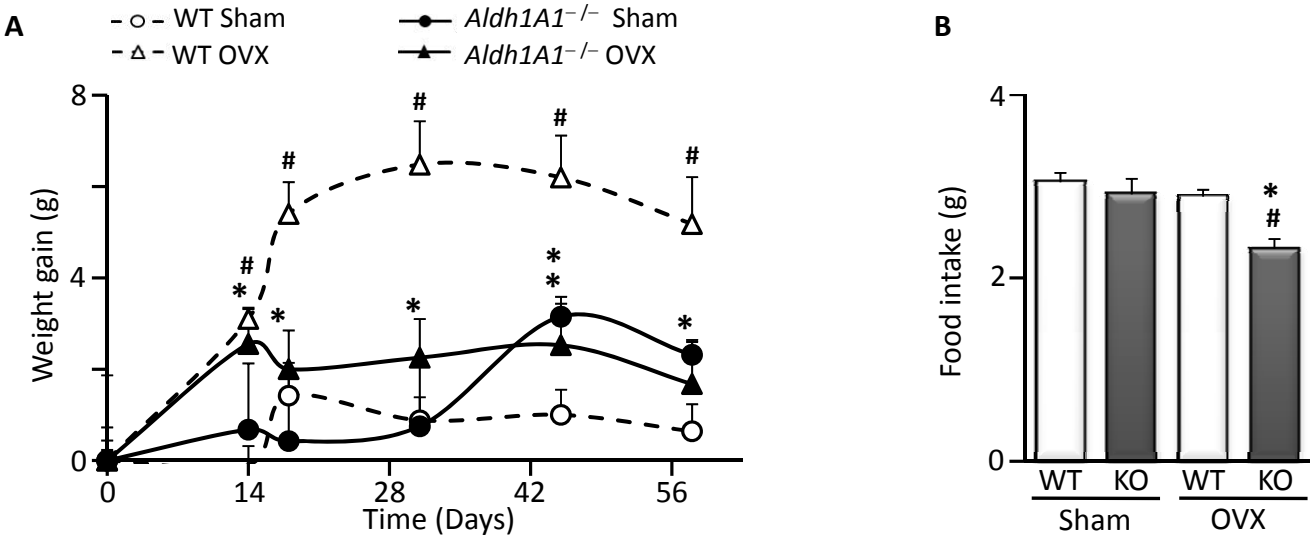

TMP ME 10 0314 FIGURE _S6

Supplementary Figure 1

Abbreviation in paper	Gene name	Ref Sequence	Species	Alias
Retinaldehyde synthesis				
Adh1	Alcohol dehydrogenase-1	NM_007409.2	m	alcohol dehydrogenase 1 (class I), ADH-AA, AI194826, Adh-1, Adh-1-t, Adh-1-t, Adh-1e, Adh-1t, Adh-3e, Adh1-e, Adh1-t, Adh1tl, Adh1tl, Adh3-e
Adh3	Alcohol dehydrogenase 7 (class IV)	NM_009626.4	m	alcohol dehydrogenase 7 (class IV), mu or sigma polypeptide, Adh3, AI325182, Adh-3, Adh-3e, Adh-3t, Adh3-e, Adh3-t, Adh4, Adt-1
Adh4	Alcohol dehydrogenase 4 (class II)	NM_011996.2	m	alcohol dehydrogenase 4 (class II), pi polypeptide, Adh2
Rdh1	Aetinol dehydrogenase 1 (all-*trans*)	NM_080436.3	m	retinol dehydrogenase 1 (all trans)
Retinaldehyde catabolism/ RA synthesis				
Aldh1a1	Aldehyde dehydrogenase family 1, subfamily A1	NM_013467.3	m	retinaldehyde dehydrogenase 1, Aldh1A1, Ahd-2, Adh2, Aldh1, Aldh1a2,E1, Raldh1
Aldh1a2	Aldehyde dehydrogenase family 1, subfamily A2	NM_009022.3	m	retinaldehyde dehydrogenase 2, Aldh1A2, AV116159, Aldh1a7, RALDH-2, Raldh1, Raldh2
Aldh1a3	Aldehyde dehydrogenase family 1, subfamily A3	NM_053080.3	m	retinaldehyde dehydrogenase 3, Aldh1A3, ALDH6, RALDH3, V1, Raldh3
Aldh8a1	Aldehyde dehydrogenase 8 family, member A1	NM_178713.4	m	Raldh4
Aldh2	Aldehyde dehydrogenase 2, mitochondrial	NM_009656.3	m	Ahd-5, Ahd5
RA-catabolism				
Cyp26a1	Cytochrome P450, family 26, subfamily a, polypeptide 1	NM_007811.1	m	cytochrome P450 26 retinoic acid A1, retinoic acid hydrolase, RAH, Cyp26, P450RA, P450RAI, MGC13860
Cyp26b1	Cytochrome P450, family 26, subfamily b, polypeptide 1	NM_175475.2	m	cytochrome P450 26B1, cytochrome P450 26 retinoic acid B1, retinoic acid B1, retinoic acid hydroxylase, CP26, P450RAI-2
Proteomic markers				
Pnpla2	Patatin-like phospholipase domain containing 2	NM_025802.2	m	adipose triglyceride lipase, desnutrin, transport-secretion protein, triglyceride hydrolase, adipose-specific tryglycerol lipase, Atgl, TTS-2.2, 0610039C21Rik, 111(
Bckdhb	Branched chain ketoacid dehydrogenase E1, beta polypeptide, Bckdhb	NM_199195.1	m	2-oxoisovalerate dehydrogenase subunit beta, BCKDHbeta
Bpnt1	3′(2′)-5′-bisphosphate nucleotidase 1	NM_011794.3	m	Bpntase, BPNT1
Casp1	caspase 1	NM_009807.2	m	ICE, Il1bc
Chmp5	Charged multivesicular body protein 5	NM_029814.1	m	chromatin modifying protein 5, RP23-28I8.4, 2210412K09Rik, AW545668
Cndp2	cytosolic non-specific dipeptidase	NM_023149.2	m	CNDP dipeptidase 2 (metallopeptidase M20 family), 0610010E05Rik, C76600, Cn2, Dip-2, Pep-1, Pep1, Carnosinase-2
Glod4	Glyoxalase domain-containing protein-4	NM_026029.2	m	1700082G03Rik, 2700085E05Rik, C81254, RP23-147P4.6
Gmfb	glia maturation factor, beta	NM_022023.1	m	GMFbeta, C79176, AI851627, D14Ertd630e, 3110001H22Rik, 3110001O16Rik
Nid1	Nidogen 1	NM_010917.2	m	A630025O17, Nid, entactin, entactin-1, nidogen-1
Prdx6	Peroxiredoxin 6	NM_007453.3	m	1-cysPrx, 9430088D19Rik, AA690119, Aop2, Aop2-rs3, Brp-12, CP-3,GPx, KIAA0106, Ltw-4,Ltw4, Lvtw-4, ORF06, Prdx6-rs3, aiPLA2, mKIAA0106
Lcp1	Lymphocyte cytosolic protein 1	NM_008879.3	m	plastin 2, lymphocyte cytosolic protein 1, AW536232, D14Ertd310e, L-fimbrin, Pls2
Ces3	Carboxylesterase 3	NM_053200.2	m	triacyl glycerol lipase, TGH
Serpina3k	Serine (or cysteine) peptidase inhibitor, clade A, member 3K	NM_011458.2	m	1300001I07Rik, D12Rp54, MMCM2, MMSpi2, RP54, Spi-2, contrapsin, SPA3K, serine protease inhibitor A3K precursor
Adipogenesis markers				
Fabp4	Fatty acid binding protein 4, adipocyte	NM_024406.2	m	422/aP2, ALBP/Ap2, Ap2, Lbpl
Pparg	Peroxisome proliferator activated receptor gamma	NM_011146.3	m	Nr1c3, PPARgamma, PPAR-gamma, PPARgamma2, PPAR-gamma2